



Jomo Kenyatta University of Agriculture and Technology

College of Engineering and Technology

School of Mechanical, Materials, and Manufacturing Engineering

Department of Mechatronic Engineering

Design and Fabrication of an Automated Discharge Collection Unit for the Synthetic Hydro-experimental Machine.

FYP-18-03

INTERIM REPORT

Juma Joel Mwimali (ENM221-0060/2017)

Kipng'eno Erick (ENM221-0068/2017)

Supervisor

Dr. Anthony Muchiri

August, 2022

Submitted in partial fulfillment of the requirements for the degree of Bachelor of Science in
Mechatronic Engineering in Jomo Kenyatta University of Agriculture and Technology, 2022

Declaration

We hereby declare that the work contained in this report is original; researched and documented by the undersigned students. It has not been used or presented elsewhere in any form for award of any academic qualification or otherwise. Any material obtained from other parties have been duly acknowledged. We have ensured that no violation of copyright or intellectual property rights have been committed.

1. Juma Joel Mwimali

Signature..... Date.....

2. Kipng'eno Erick

Signature..... Date.....

Approved by:

Supervisor: Dr. Anthony Muchiri

Signature..... Date.....

Contents

Declaration	I
Table of Contents	V
List of Figures	V
Nomenclature	IX
Abstract	IX
1 Introduction	1
1.1 Background	1
1.2 Problem statement	1
1.3 Objectives	2
1.3.1 Main objective	2
1.3.2 Specific objectives	2
1.3.3 Expected outcomes	2
1.4 Justification	3
2 Literature Review	4
2.1 Introduction	4
2.2 Existing Technologies	4
2.2.1 Computational Fluid Dynamics	4
2.2.2 Analytical Predictions	7
2.3 Related Works	9
2.3.1 Electromagnetic activation	9
2.3.2 Pneumatic Control	10
2.4 Summary	11
2.5 Gap analysis	11

3 Methodology	13
3.1 Overview	13
3.2 Discharge flow control unit	13
3.2.1 Flow control sub-unit	13
3.2.2 Flow diversion sub-unit	39
3.2.3 Electrical	50
3.2.4 Software and control	52
3.3 Discharge Handling Unit	54
3.3.1 Discharge collection tank sub-unit	54
3.3.2 Outlet valve sub-unit	60
3.3.3 Weight measurement sub-unit	61
3.3.4 Temperature measurement sub-unit	65
3.3.5 Electrical	66
3.3.6 Software and control	68
3.4 Interface and Control Unit	68
3.4.1 Interface sub-unit	68
3.4.2 Controller sub-unit	72
3.4.3 Electrical	75
3.4.4 Software and control	76
4 Results	78
4.1 Discharge Flow Control Unit	78
4.1.1 Flow control sub-unit	78
4.1.2 Flow diversion sub-unit	78
4.1.3 Unit Assembly	78
4.2 Discharge Flow Handling unit	80
4.2.1 Discharge collection tank sub-unit	80
4.2.2 Outlet valve sub-unit	80
4.2.3 Weight measurement sub-unit	80

4.2.4	Temperature measurement sub-unit	80
4.2.5	Final assembly	81
4.3	Budget	82
5	Conclusion	83
References	84
Appendices	87
A Appendix	87
A.1	Semester 1 Time Plan	87
A.2	Semester 2 Time Plan	89
A.3	P16-S Micro linear actuator	89
A.4	Synthetic Hydro Experimental Machine in JKUAT	90

List of Figures

Figure 2.1	Test loop schematic	5
Figure 2.2	Experimental setup	6
Figure 2.3	Venturi Meter	7
Figure 2.4	Sampler actuation mechanism	10
Figure 2.5	Dispensing mechanism	10
Figure 3.1	Current discharge control unit	13
Figure 3.2	Nema 17 Stepper motor	15
Figure 3.3	Nema 17 Stepper Motor Drawing	16
Figure 3.4	Interface	17
Figure 3.5	Motor Cage	18
Figure 3.6	Ball valve socket	19
Figure 3.7	Mounting straps	20
Figure 3.8	Stepper Actuated ball valve	21
Figure 3.9	Simulation results	23
Figure 3.10	MG996R servo motor	25
Figure 3.11	Servo motor cage	27
Figure 3.12	Servo motor mounting plate	28
Figure 3.13	Servo motor mounted assembly	29
Figure 3.14	Spur gear	30
Figure 3.15	Servo motor with spur gears	31
Figure 3.16	Mounting rods	33
Figure 3.17	Interface	34
Figure 3.18	Top strap	35
Figure 3.19	Bottom strap	35
Figure 3.20	Servo motor discharge flow control assembly	36
Figure 3.21	Servo Assembly simulation results	38
Figure 3.22	Xeryon-XLA Series 3 piezo actuator	40

Figure 3.23 P16S linear actuator	41
Figure 3.24 Electromagnetic actuator holder	42
Figure 3.25 Diversion flap	43
Figure 3.26 Flap support frame	44
Figure 3.27 Crank	45
Figure 3.28 Coupler	46
Figure 3.29 Rocker	47
Figure 3.30 Flow Diversion assembly	48
Figure 3.31 Diversion assembly FEA results	49
Figure 3.32 Servo Connection	50
Figure 3.33 Electromagnetic Actuator circuit	51
Figure 3.34 IRF520 Module	52
Figure 3.35 Cuboid discharge container	55
Figure 3.36 Horizontal Cylindrical tank	56
Figure 3.37 Tank simulation results	57
Figure 3.38 Cylindrical tank support frame	58
Figure 3.39 Collection tank	59
Figure 3.40 Butterfly valve	60
Figure 3.41 Solenoid valve	61
Figure 3.42 Ultrasonic sensor measurement model	63
Figure 3.43 Strain-type load cells	64
Figure 3.44 Collection tank with load cells	64
Figure 3.45 DS18B20 temperature probe	65
Figure 3.46 Load cells circuit	67
Figure 3.47 LCD with keypad	70
Figure 3.48 LCD with touch	70
Figure 3.49 Lcd with knob	71
Figure 3.50 GUI interface	72
Figure 3.51 Board Selection	73

Figure 3.52 Load cells circuit	75
Figure 3.53 STM32 connected with LCD	75
Figure 3.54 Application logic	76
Figure 4.1 Unit Exploded view	79
Figure 4.2 Final Assembly	81
Figure A.1 P16-S Micro linear actuator dimensions	89
Figure A.2 S.H.E.M relevant machine dimensions	90

List of Tables

Table 2.1	Calculated C_d	5
Table 2.2	Results	7
Table 3.1	Nema 17 Stepper Motor Technical specification	16
Table 3.2	MG996R Servo motor specifications	24
Table 3.3	XLA series 3 piezo actuator specifications	40
Table 3.4	P16-S Micro-linear actuator technical specifications	41
Table 3.5	DS18B20 temperature range specifications	65
Table 4.1	Budget	82
Table A.1	Semester 1 timeplan	87
Table A.2	Semester 2 Timeplan	88

Abstract

The synthetic hydro experimental machine used for fluid mechanics experiments in the fluids lab at JKUAT employs an older technology in the measurement of fluid properties. The machine is wholly mechanical as most of the parameter manipulations are done by hand. In experiments to determine the coefficient of discharge by using the Venturi and the Orifice, flow rate control is achieved by hand by opening the ball valve in small steps which can be inconsistent. Besides, one has to measure the temperature and time of discharge simultaneously. As a result, with these discrepancies and lack of synchronism, the findings might frequently be outside of the acceptable range due to human error.

This project intends to design and fabricate an automated discharge collection process to minimize human error while maintaining the credibility of the experiment. A modular system has been designed comprising of three major units; the discharge flow control unit, discharge handling unit and the interface and control unit. Through the use of a graphical user interface, the user will be prompted to input the time to perform the experiment and the number of steps. Based on the provided information and the pipe circumference, the system automatically determines the number of steps required. The system will automatically initiate the pump to force water into the pipe system for a specified amount of time to attain steady flow after which the ball valve closes. A servo motor attached to the valve shaft is used to open the valve in small and precise steps. A flap system diverts the discharge either into the collection tank or into the water reservoir. The collected discharge is weighed and at the same time, its temperature is measured, recorded, and displayed on the user interface after which the discharge is released into the reservoir through a solenoid valve to allow for the next step.

This automation will reduce the huge error margins in fluid flow experiments due to human errors.

1 Introduction

1.1 Background

Fluid flow measurement involves the measurement of the properties of a smooth and uninterrupted stream of flowing particles that conform to a pipe. These flow properties include the coefficient of discharge, mass flow rate, fluid velocity, differential pressure, and conductivity coefficients [1]. They are altered and measured by flow measuring devices such as the Venturi, the Orifice, turbine flow meters and rotameters [2]. These measurements are finally related to the flow using the Bernoulli's equation.

The Synthetic Hydro-Experimental machine, currently installed in JKUAT, is a configurable machine with these flow meters. This machine is used to conduct experiments to establish relationships between the fluid flow properties and the behavior of the flow. It has a lift pump, gate valves, alcohol manometers, pressure gauges, a Pelton turbine, a Venturi, an orifice, and water reservoirs. During experiments, the lift pump is turned on, and the discharge valve is fully opened to establish a steady flow. The discharge valve is then closed. The valve is opened in small steps depending on the number of steps required. For each step, the discharge is collected, and its temperature is measured within a specific time interval. Finally, the weight of the collected discharge is also measured.

1.2 Problem statement

In fluid flow experiments utilizing the Venturi and the orifice to establish the coefficient of discharge, the discharge steps must be precisely opened, and time and temperature measurements must be made concurrently with discharge collection so as to achieve values that are within a reasonable range. The Synthetic Hydro-Experimental machine now in use at JKUAT to establish this relationship, however, is entirely mechanical, making it impossible for a human to do some of the simultaneous measurements. A ball valve regulates the flow rate in small intervals using human intuition, which can be imprecise.

As a result, with these discrepancies, the findings might frequently be outside of the acceptable range. Automating the discharge collection process can minimize the error in the results and still preserve the credibility of the experiment.

1.3 Objectives

1.3.1 Main objective

To automate the discharge collection process for the Synthetic Hydro-Experimental machine.

1.3.2 Specific objectives

1. To design an automated discharge flow control unit that can precisely discharge in steps.
2. To design and fabricate a discharge collection unit with automated weight, time and temperature measurements.
3. To design a user interface and the control algorithm.

1.3.3 Expected outcomes

1. Discharge flow control unit

A discharge flow control mechanism that can turn the ball valve in precise steps. The steps obtained from the division of the circumference of a full turn by the number of steps should be precise to the nearest whole number.

2. Discharge Handling unit

A discharge collection unit that can precisely collect the discharge within the specified time interval while taking its temperature and weight simultaneously. This can be expected if the expectations of the following sub-units are met :

(a) Flow diversion sub-unit

A precisely sized diversion sub-unit, correctly positioned to collect or divert the discharge with minimal splashes the whole stream. This will improve on the accuracy of the weight of the discharge and hence that of the whole experiment experiment in general.

(b) Discharge collection tank

A discharge collection tank whose shape can allow for accurate weight measurement. The collection tank should allow for motivated discharge into the reservoir and it should also be positioned in such a way that flow into this tank utilizes gravity to eliminate the need for an extra pump.

(c) Discharge weight and temperature measurements

It is expected these units measuring devices can measure to the smallest resolution.

3. Interface and Control Unit

The control module that can handle intense computations such as error approximation, immediate rendering of results and communicating with the sensors and transducers that will be used in the system. The user interface should also be slick and ergonomic.

1.4 Justification

This automation will streamline the discharge collecting process while also ensuring the consistency and quality of the data collected in each phase of the fluid flow tests performed on the system. In contrast to the existing condition, such automation allows a single person to perform the experiment without significant effort. Furthermore, the automated system will also be modular, allowing it to be readily attached and detached from the main machine with few modifications.

2 Literature Review

2.1 Introduction

Fluid flow experiments involve determination of the flow velocity, the mass flow rate or volumetric flow rate. These experiments are used to familiarize the students with typical methods of flow measurement of an incompressible fluid and, at the same time demonstrate applications of the Bernoulli's equation. Thus, these experimental investigations require the application of measuring techniques to yield quantitative information on the relationship between pressure, temperature and local flow velocities.

2.2 Existing Technologies

Some advanced and even rudimentary technologies have been used in place of the Synthetic Hydro-Experimental machine for the determination of fluid flow properties. The technologies include :

2.2.1 Computational Fluid Dynamics

Computational fluid dynamics(CFD) is a powerful modelling and analysis technique that utilizes finite difference techniques to solve highly non-linear differential equation of pressure, energy, relative humidity, air temperature and velocity [3]. It can be used to model fluid flow in flow measurement devices.

Tukimin et al [4] in their study conducted a CFD analysis using an Single Kernel Estimate (SKE) turbulence model to determine the coefficient of discharge of a Venturi tube, and finally compared the results to those obtained from a physical experimental setup. The test loop shown in figure 2.1 was used both in a physical setup and a CFD model.

They designed a CFD model using the ANSYS Design Modeller software. The model consists of a Venturi tube, designed according to the standards ISO 5167:2003 [5], and a

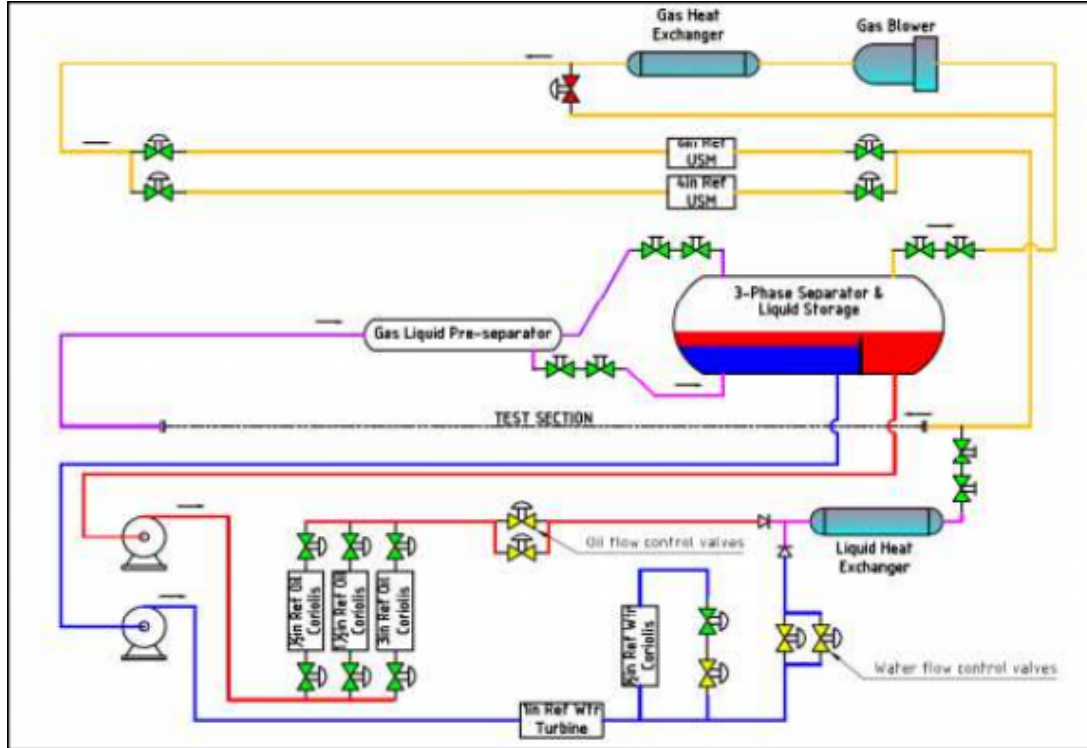


Figure 2.1: Test loop schematic by Tukimin et al [4]

Table 2.1: Calculated C_d

Venturi under Test	Average Discharge Coefficient From experiment	Average Discharge Coefficient From CFD post
Venturi 1	0.99366	0.984347

liquid and gas system. They did a physical experiment using the same test matrix used in the numerical simulation model. Finally, they computed the coefficient of discharge of the venturi using equation 2.1.

$$Cd = \frac{4m\sqrt{1 - \beta^4}}{\pi\varepsilon d^2\sqrt{200000D\rho_1\rho_1}} \quad (2.1)$$

The results obtained in 2.1 showed a difference of less than 1% between the C_d obtained

from the two setups.

Tamhankar et al [6] also did a similar experiment using a CFD model designed in ANSYS Fluent 13.0 utilizing a Realizable $k-\epsilon$ turbulence model which is superior to a Standard $k-\epsilon$ turbulence model and compared the results to those obtained from an experimental setup show in figure 2.2.

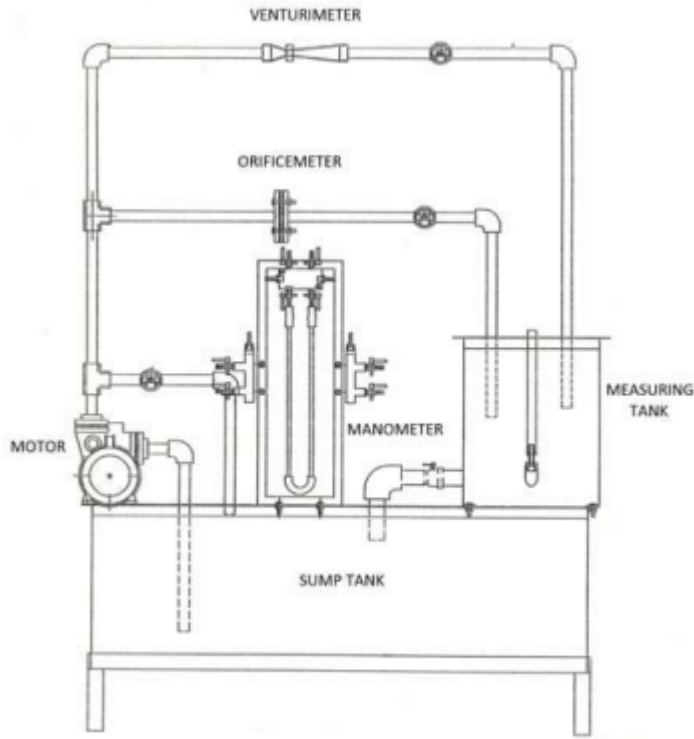


Figure 2.2: Experimental setup by Tamhankar et al [6]

Table 2.2 shows the results obtained from the study

The study concluded that difference in values of the coefficient of discharge obtained from the model and those obtained from the experimental setup was less than 5% .

Table 2.2: Results

Reading No.	Experiment	CFD analysis
1	0.9724	0.9619
2	0.9592	0.9689
3	0.9779	0.9692

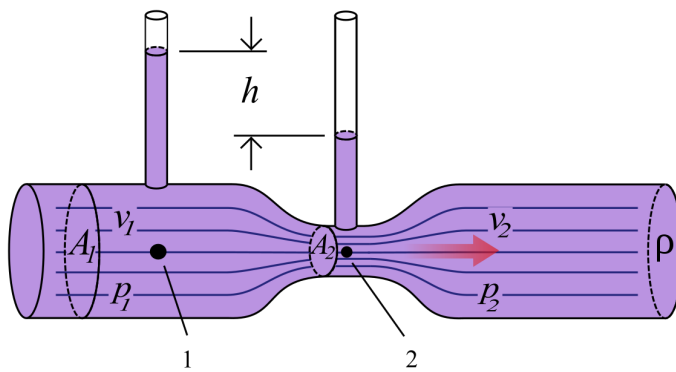


Figure 2.3: Venturi meter [7]

2.2.2 Analytical Predictions

This technique utilizes the Bernoulli's equation to establish an analytical correlation between the fluid flow and the coefficient of discharge of the Venturi meter.

Figure 2.3 shows the Venturi meter. Assuming the flow is ideal and applying the Bernoulli's equation before and after the contraction,

$$\frac{p_1}{\rho g} + \frac{v_1^2}{2g} + z_1 = \frac{p_2}{\rho g} + \frac{v_2^2}{2g} + z_2$$

But $Z_1 = Z_2$,

$$\begin{aligned} \frac{(p_1 - p_2)}{\rho} &= \frac{(v_2^2 - v_1^2)}{2} \\ \frac{(p_1 - p_2)}{\rho} &= \frac{v_2^2}{2} \left(1 - \frac{A_2^2}{A_1^2}\right) \\ \frac{\Delta p}{\rho} &= \frac{v_2^2}{2} (1 - \beta^4) \\ v_2 &= \frac{1}{\sqrt{1 - \beta^4}} \sqrt{\frac{2\Delta p}{\rho}} \end{aligned} \tag{2.2}$$

Applying the continuity equation to the result of the derivation in 2.2,

$$\begin{aligned} Q_{th} &= A_1 v_1 = A_2 v_2 \\ Q_{th} &= A_2 v_2 = \frac{1}{\sqrt{1 - \beta^4}} \frac{\pi d^2}{4} \sqrt{\frac{2\Delta p}{\rho}} \end{aligned} \tag{2.3}$$

Equation 2.3 of theoretical flow rate is based on the assumption that the flow is steady, incompressible, inviscid, irrotational, no losses and the velocities V_1 and V_2 are constant across the cross section [8].

$$Q_{act} = \frac{C_{dstd}}{\sqrt{1 - \beta^4}} \frac{\pi d^2}{4} \sqrt{\frac{2\Delta p}{\rho}} \tag{2.4}$$

The frictional and viscous losses in a laminar flow can be estimated by the Darcy's law

$$H_L = \frac{(\Delta p)_{viscous}}{\rho g} = f \frac{v^2}{2 g D} \tag{2.5}$$

where 'f' is the friction factor.

Coefficient of discharge equation 2.7 where for laminar flow, 'f' is given by equation 2.6 . This equation is derived from both the Darcy's law equation and the theoretical flow rate equation 2.3.

$$f = \frac{64}{R_{ed}} \tag{2.6}$$

$$C_d = 0.995 \sqrt{\frac{1}{(1 + 3f)}} \quad (2.7)$$

Arun et al [8] did a comparision of the C_d obtained by this method and that obtained from a CFD simulation. The study concluded that the results from the two methods had an uncertainty of 0.9%.

2.3 Related Works

Discharge collection techniques have been developed for various applications. Some of these applications are related to the discharge collection unit used in the Synthetic Hydro-Experimental machine.

2.3.1 Electromagnetic activation

Angelo et al [9] implemented this technique in the design and testing of an Modular Automatic Water Sampler(MAWS). They designed MAWS and mount them on unmanned marine vehicle with the aim of collecting water samples for scientific campaigns in front of polar tidewater glaciers. Their main design considerations was the response time of the stopper since the MAWS were operated under water and at the risk of damage by glaciers. The actuation unit of the sampler is shown in figure 2.4.

When the coil in the solenoid is crossed by a current a strong magnetic field is generated that attracts the ferromagnetic plunger connected to the sealing stopper and opens the bottle allowing water to flow into the bottle's neck. As the current stops the two permanent magnets attract each other and the stopper seals the bottle [9].

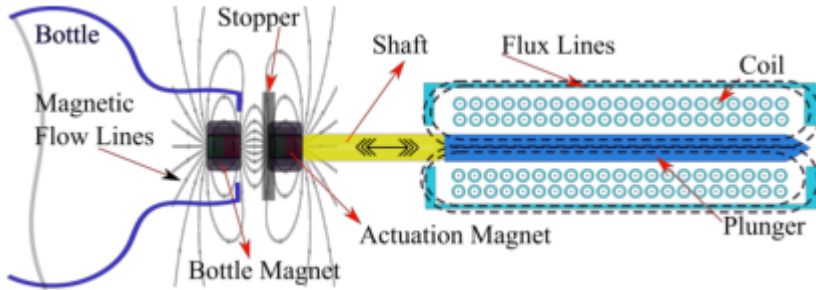


Figure 2.4: Sampler actuation mechanism [9]

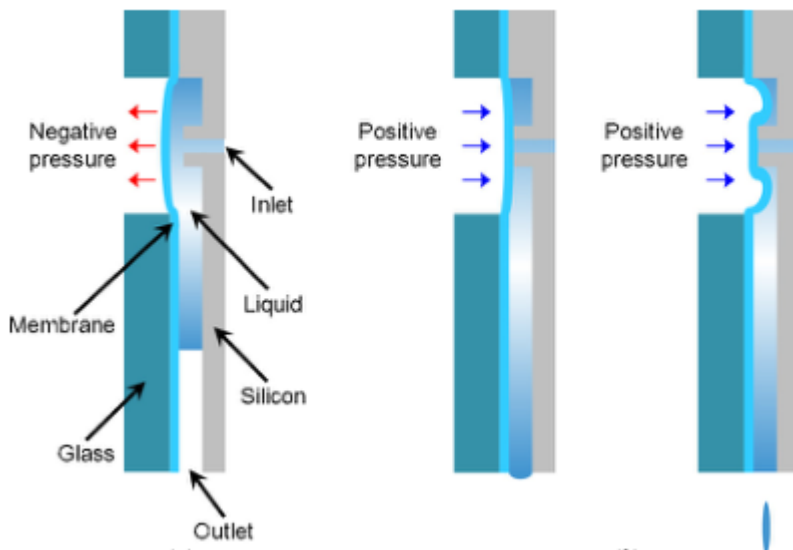


Figure 2.5: Dispensing mechanism [10]

2.3.2 Pneumatic Control

Pneumatic actuators utilize the power of compressed air to impart motion on objects. Sangmin, and Joonwon [10] did a design of cartridge-type pneumatic dispenser with a back flow stopper. The system used a membrane covering a discharge hole. The membrane was opened and closed using negative and positive pneumatic pressure respectively as shown in figure 2.5.

The application was able to do precise dispensation of 100nL to 400nL droplets.

2.4 Summary

Every fluid flow experiment done on the Synthetic Hydro-Experimental machine involves the collection of discharge and the measurement of its properties. The most common experiment is the determination of the coefficient of discharge of the Venturi and the Orifice. In this literature, other techniques such as CFD and analytical methods have been found to be effective as alternatives to this machine. These techniques have been proven to produce results with a difference of less than 1% from the experimental results obtained from a physical setup. Such results can also be obtained from the fluids rig currently used in JKUAT by automating the discharge collection unit. With regard to this, the literature has also covered discharge collection techniques that have proven to be effective in other applications and can be adapted for this automation. This techniques include the application of pneumatics and electromagnetism.

2.5 Gap analysis

1. The use of the CFD method or the analytical method undermines the credibility of the fluid flow experiments. This two techniques are rather used for the design of fluid flow measuring devices.
2. CFD method can also be very resource intensive in terms of compute resources. Softwares used for this method requires a hefty license fee.
3. The application of the analytical method involves tedious calculations and several assumptions which can produce untrustworthy results.
4. The use of the Synthetic Hydro-Experimental machine with a manual discharge collection unit often produce results with huge error margins.

This project proposal is entirely focused on addressing gap number four with the application of techniques such as pneumatics or electromagnetism. This closes in the techno-

logical gap with the use of CFD, and simplify the use of analytical methods by providing data for the computation of fluid flow properties.

3 Methodology

3.1 Overview

This project consists of three main units: a discharge flow control unit, a discharge handling unit, and a software and control unit.

3.2 Discharge flow control unit

This unit consist of two main sub-units:

1. Flow control sub-unit

This sub-unit controls the dispensing of the flow from the discharge pipe in steps.

2. Flow diversion sub-unit

This sub-unit diverts the flow from the main discharge pipe either to the discharge collection tank or to the main reservoir.

3.2.1 Flow control sub-unit

The current state-of-art of this unit is as shown in Figure 3.1.



Figure 3.1: Current discharge control unit

The $1\frac{3}{4}$ inch ball valve on the main discharge pipe is opened in steps by hand using the lever. The size of a step is determined by intuition.

Design

To ensure minimum modification of the existing machine, the automation of this unit utilized the existing ball valve. The opening and closing of the valve is automated using a motorized system that can open the valve in precise steps.

Motor

The selection and the sizing of the motor for this application was based on the following considerations:

1. The torque required to open and close the ball valve.
2. The steps size or the number of steps the system can open the valve.

Based on these two considerations, the following two applications were feasible.

1. Stepper Motor

This motor operates by accurately synchronizing position with the pulse signal output from the controller to the driver thus achieving highly accurate positioning and speed control. Stepper motors feature high torque and low vibration at low speeds ideally below 1500rpm, ideal for applications requiring quick fixed positioning in a short distance [11]. Furthermore, stepper motor rotates with a fixed step angle typically 1.8 degrees for a 2-phase. However, to achieve this requires the use of a micro-step driver.

Besides having full control of rotation and speed, the simple structure of stepper motors is achieved without using electrical components, such as an encoder within the motor. For this reason, stepper motors are very robust and have high reliability with very few failures. As for stopping accuracy, $\pm 0.05^\circ$ (without cumulative

pitch errors) is very accurate [11]. Because the positioning of stepper motors is performed by open-loop control, and operated by the magnetized stator and magnetic rotor with small teeth, stepper motors have a higher follow-up mechanism toward commands than the servo motors. Also, no hunting occurs when stopping it.

Design with stepper motor

(a) Motor selection

From the stepper motors available in the market, Nema 17 Stepper motor shown in figure 3.2 was the best choice for the job since it can produce a 1.8^0 step out of the box without a microstep driver. With the help of a microstep driver, it can produce as small as 1^0 step.



Figure 3.2: Nema 17 Stepper motor [12]

Its technical specifications are as shown in the table below:

Property	Value
Rated Voltage	12V DC
Current	1.2A at 4V
Step Angle	1.8 deg
No. of Phases	4
Motor Length	1.54 inches
4-wire, 8 inch lead	
steps per revolution	200
Operating Temperature	-10 to 40 °C
Unipolar Holding Torque	22.2 oz-in
Maximum torque	4.8 Kg.cm

Table 3.1: Nema 17 Stepper Motor Technical specification [12]

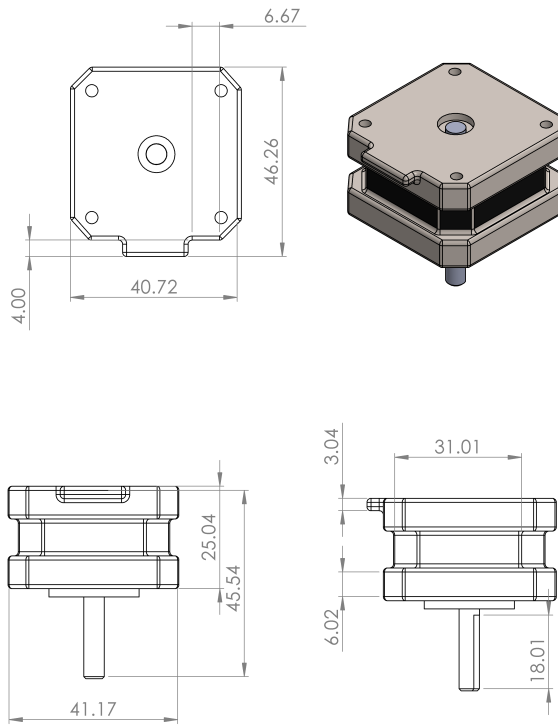


Figure 3.3: Nema 17 Stepper Motor Drawing

Figure 3.3 shows the actual dimensions of a nema 17 stepper motor.

(b) Ball valve - motor interface

An interface is required to connect the motor rotor to the ball valve. There were two option for this application:

- An interface that could fit the rotor on one end and with claw-like fingers on the other end to turn the existing ball valve's lever.
- An interface that could fit the rotor on one end and with the other end, similar to the lever, that could be used in place of the lever.

The second option was chosen since the first choice will introduce a lag in a turn action since the point of action on the lever is displaced from the line of rotation of the rotor.

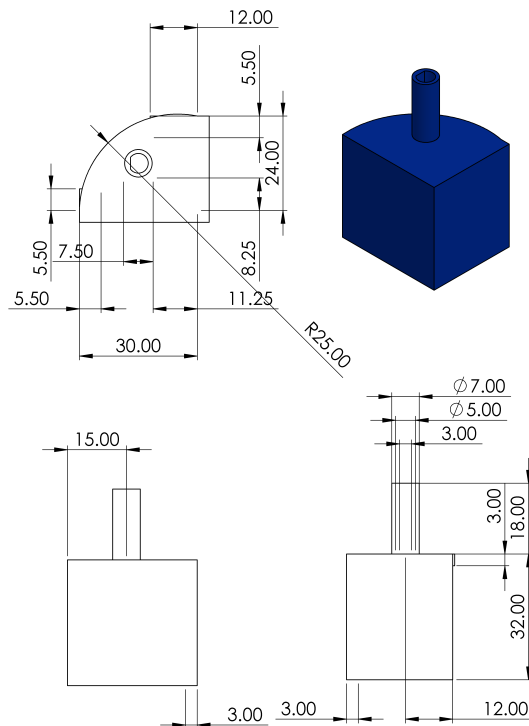


Figure 3.4: Interface

Figure 3.4 shows the interface design. Dimensions of the interface, such as the width of its base, were measured and transferred from the existing lever.

(c) Motor cage

In order to support the motor on the ball valve, a motor cage was designed to fit the motor as shown in Figure 3.5.

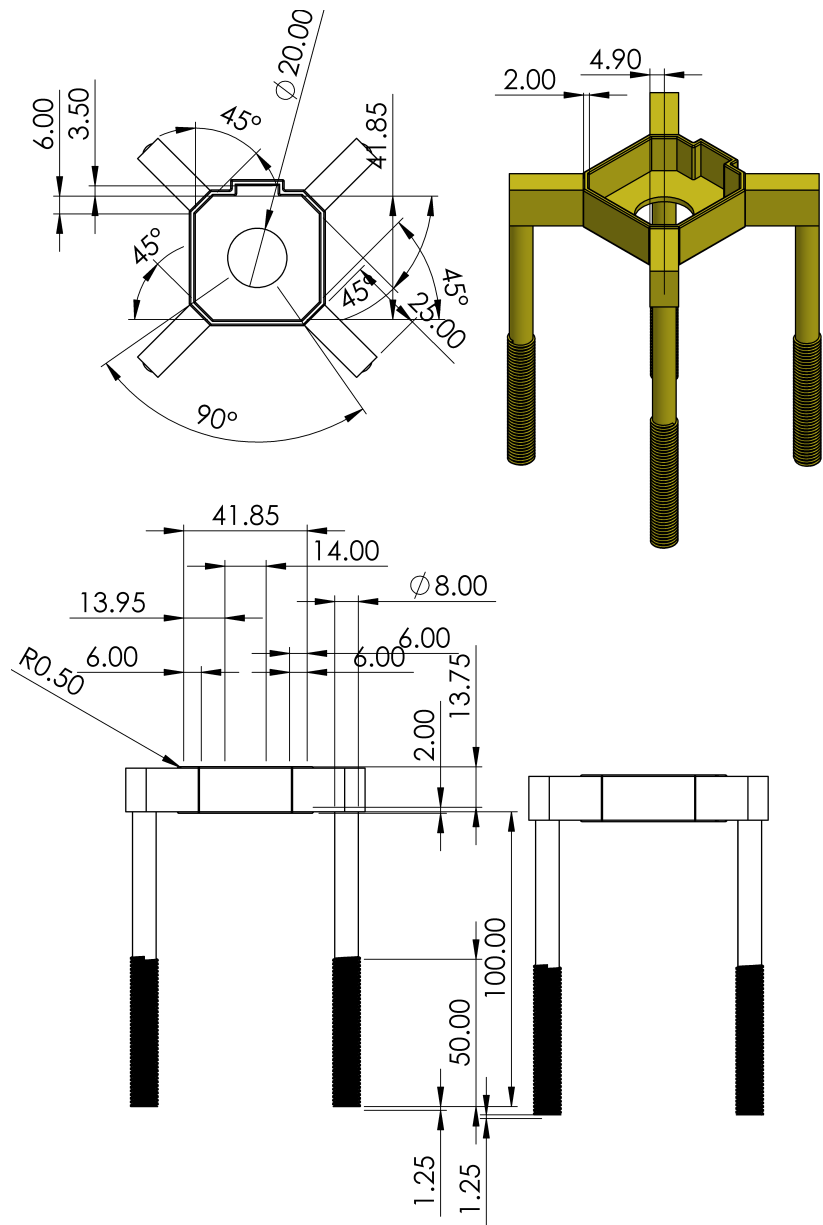


Figure 3.5: Motor Cage

The dimensions of the motor cage in figure 3.5 were determined from that of the stepper motor, the motor-ball valve interface, and that of the ball valve socket shown in figure 3.6.

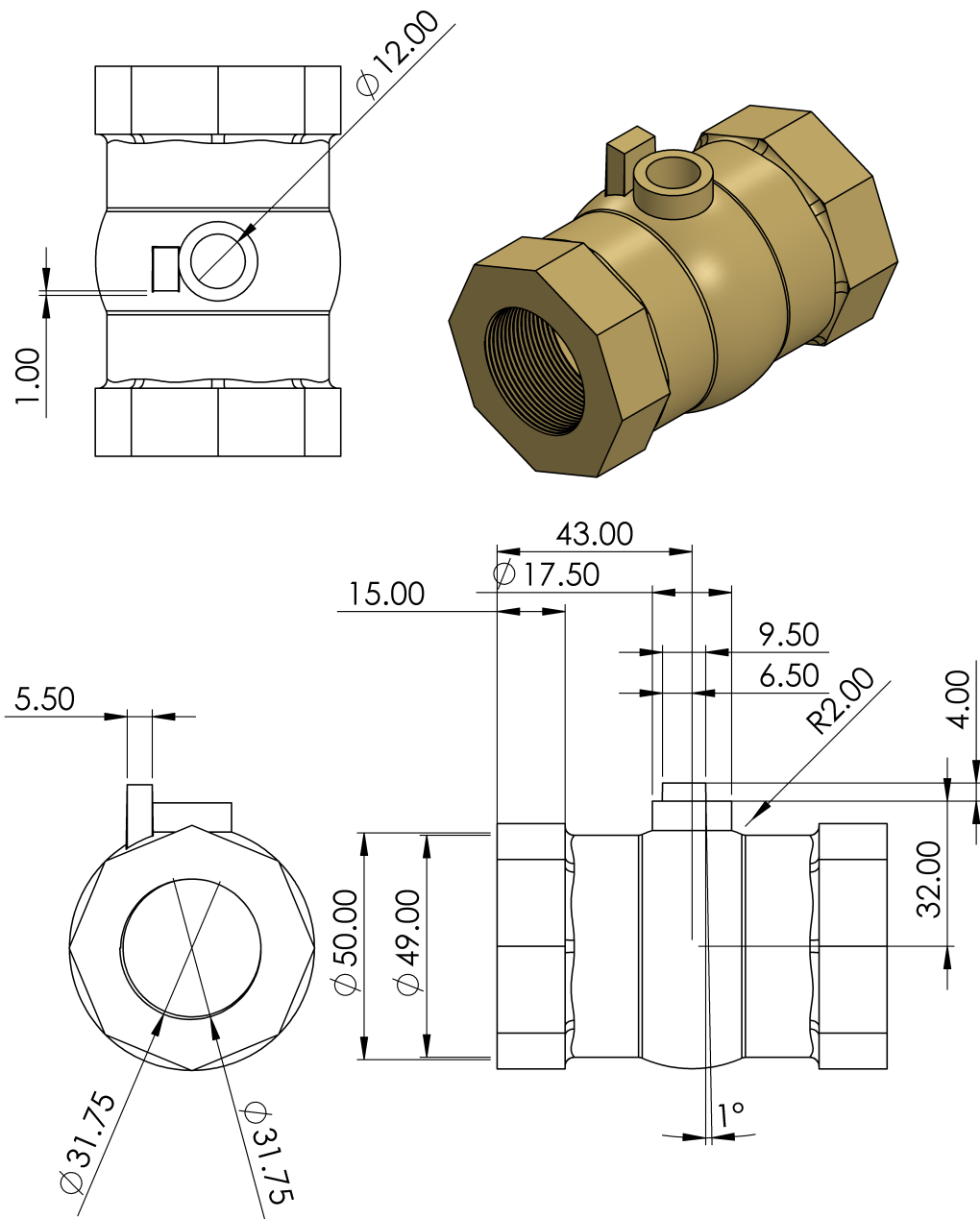


Figure 3.6: Ball valve socket

(d) Straps

The motor cage with the stepper motor mounted is mounted on the main discharge pipe using straps, one of which is shown in figure 3.7.

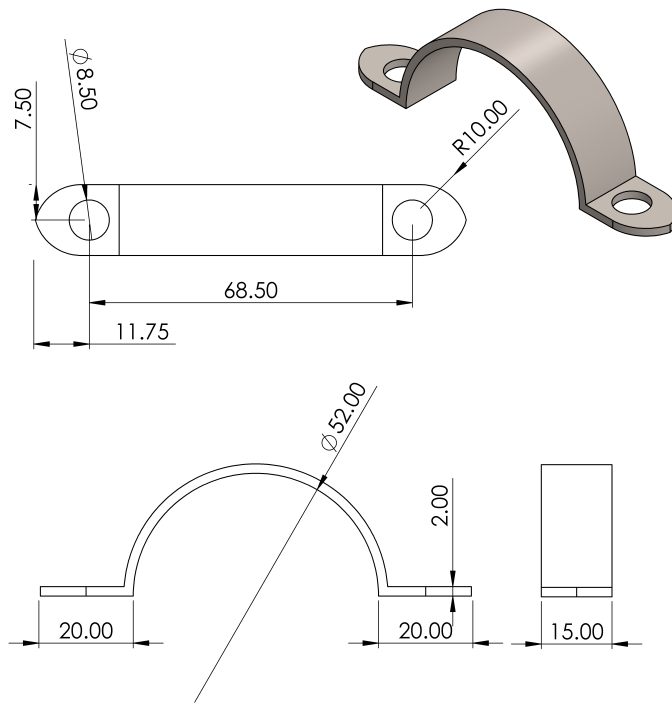


Figure 3.7: Mounting straps

(e) Assembly of discharge flow control using stepper

The assembly of the discharge control unit is as shown in figure 3.8. Nuts are used to fasten the whole structure on the main discharge pipe.

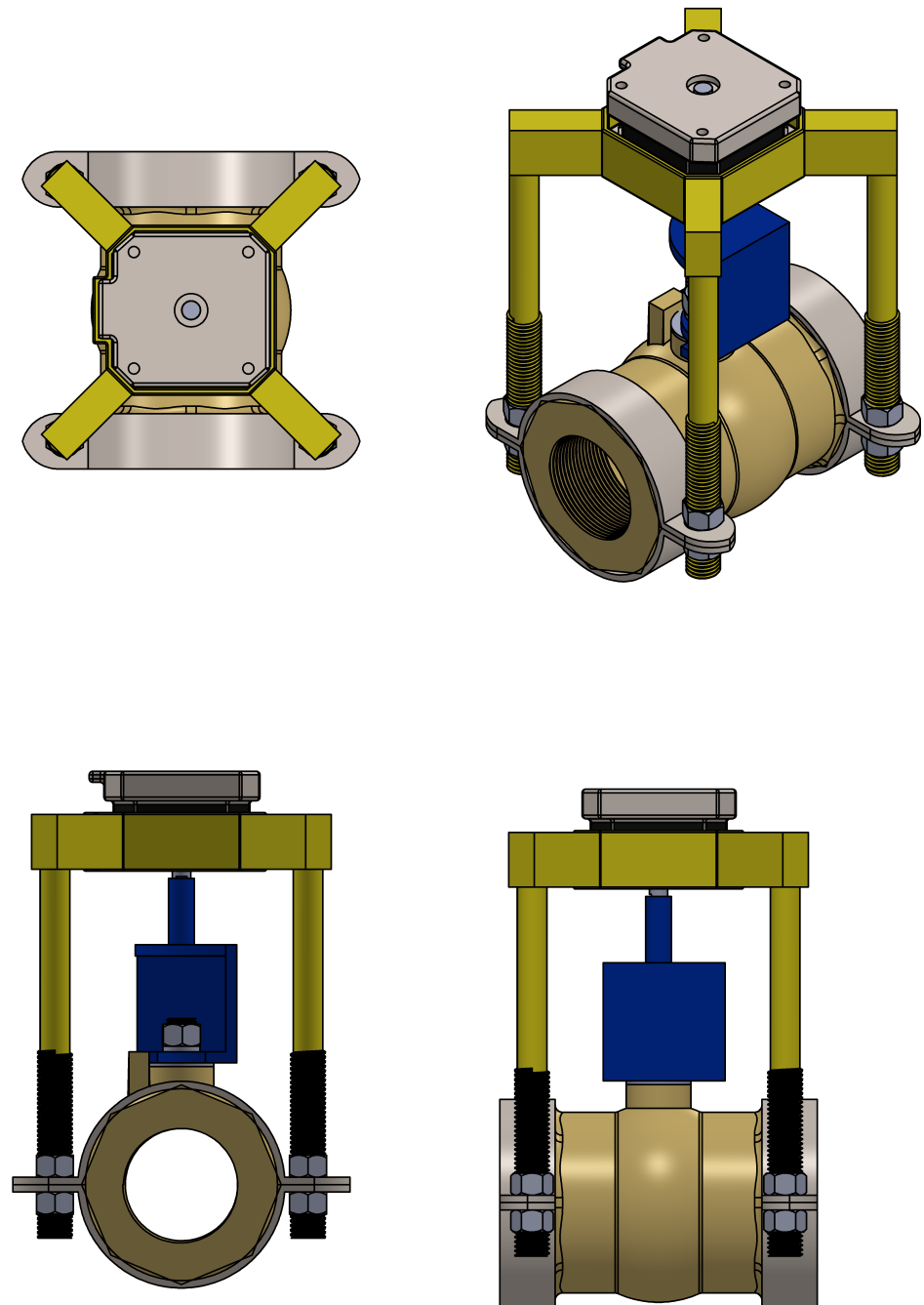


Figure 3.8: Stepper Actuated ball valve

(f) Finite element analysis of the assembly

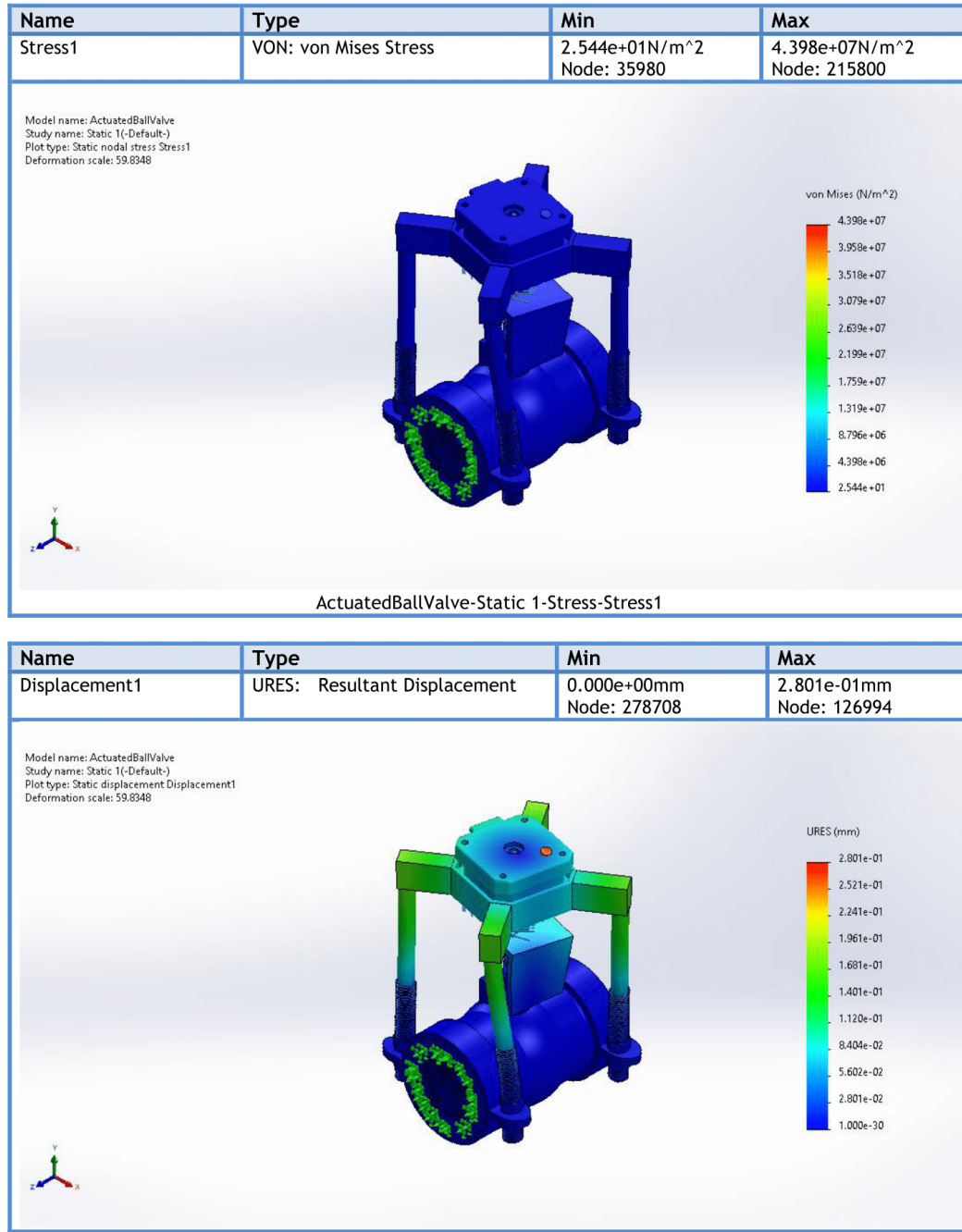
The assembly was stress tested by applying a torque on the motor cage to determine if it could hold at the maximum torque of the motor. To do this, each part of this assembly will be assigned a material. Polyactic acid (PLA) was selected as the common material for all of the parts in the assembly. This is majorly due to the following reasons:

- The maximum weight of the part to be supported by the structure is the stepper motor's weight, 450 grams. This can be supported by a 3D printed plastic support. A lighter material such as fiber glass or carbon fiber could be used but they are costlier than the set project's budget.
- The parts are complex for fabrication on the currently existing machinery in the university.

(g) Results

As shown in figure 3.9, the structure holds for the maximum torque of a Nema 17 stepper motor, $4.9kg.cm$ or $0.4707192Nm$.

Study Results



SOLIDWORKS

Analyzed with SOLIDWORKS Simulation

Simulation of ActuatedBallValve

13

Figure 3.9: Simulation results

2. Servo Motor

Servo motors run significantly faster than stepper motors, with speeds greater than 1500 rpm [13]. This enables servomotors to be used with gearboxes to deliver much higher torque at useful speeds. They also deliver more consistent torque across the speed range of the motor. Unlike stepper motors, they do not have holding torque. Closed-loop operation enables the controller/drive to command that the load remain at a specific position, however, and the motor will make continual adjustments to hold it there. Thus, servomotors can produce de facto holding torque [13]. The Servo motor rotates with a fixed step angle as low as 1 degree with or without the use of a driver. Furthermore, when powered, servomotors tend to move their shaft position to zero, a phenomenon known as hunting.

Design with servo motor

(a) Motor selection

An MG996R Servo motor shown in figure 3.10 was the best choice among many servo motors found in the market. It is the motor that provided the torque required to turn the ball valve at an optimum price for the project's budget.

The motor specification as shown in table 3.2.

Property	Value
Operating Voltage	+5V
Current	2.5A (6V)
Stall Torque	9.4 kg/cm (at 4.8V)
Maximum Stall Torque	11 kg/cm (6V)
Operating speed	0.17 s/60°
Gear Type	Metal
Rotation	0°-180°
Weight of motor	55gm

Table 3.2: MG996R Servo motor specifications [14]

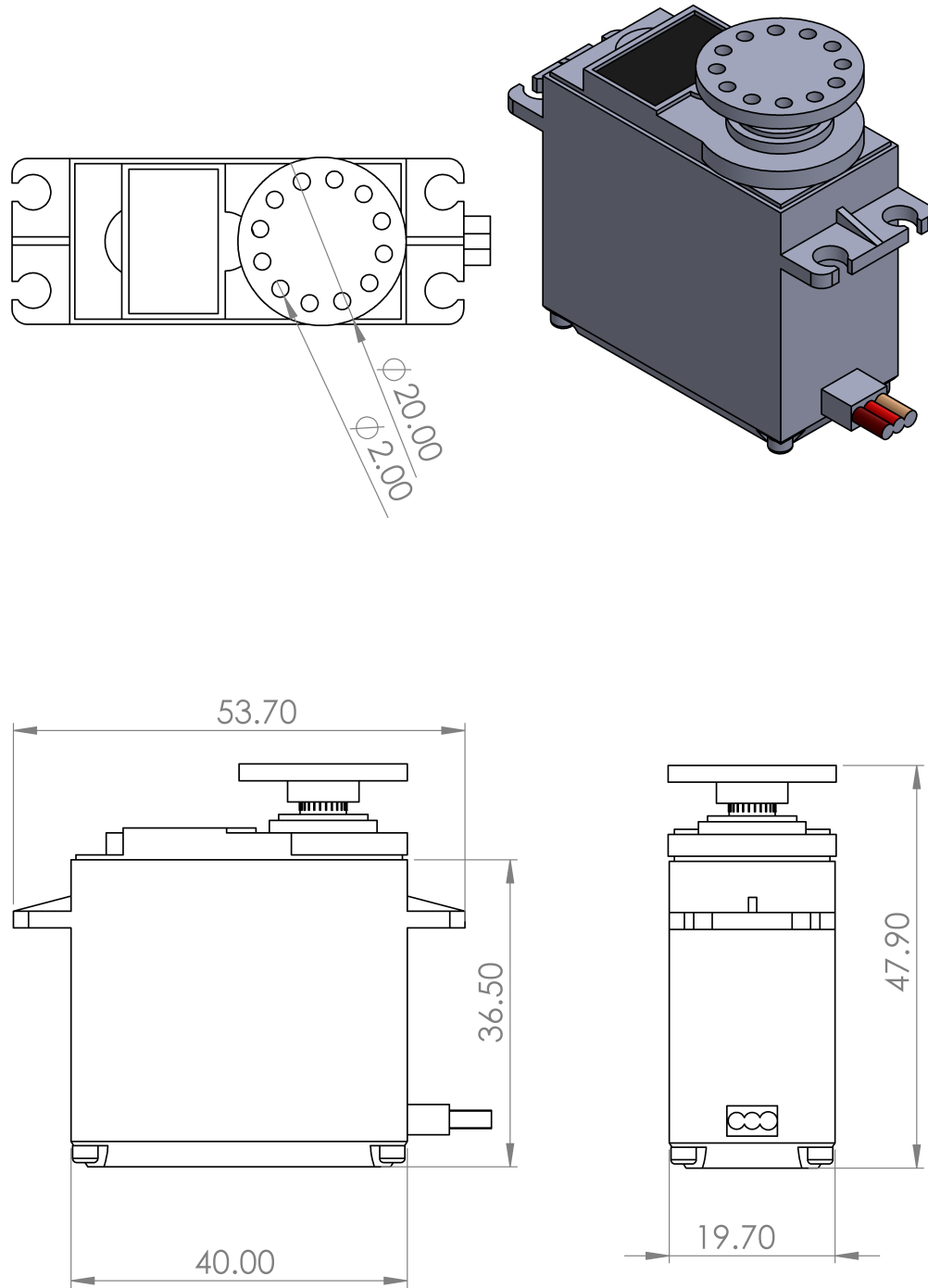


Figure 3.10: MG996R servo motor

The mounting mechanism of a servo motor is not as direct as that of the stepper motor since a servo motor homes to 0^0 on powering. It is required that the home position of the servo motor is equal to the closed position of the ball valve. Therefore, during mounting, the servo motor must be rotated to align its home position with the closed position of the ball valve.

The mounting mechanism should therefore allow for this rotation. A cuboid cage could have been used to support the motor in place, but since the centre of mass of this motor is displaced from its line of axle rotation, rotating the cuboid could mean repositioning the support stands for the cuboid.

There were two options that could achieve this kind of rotation:

- i. A combination of a cuboid cage on a circular plate. The cuboid cage could hold the motor while the plate allows the rotation of the assembly of the two without the need of repositioning the stands holding the assembly on the ball valve.

Designs with this approach

- **Servo motor cage**

The cage shown in figure 3.11 is screwed on to the motor flaps. It just adds additional mounting points for the motor.

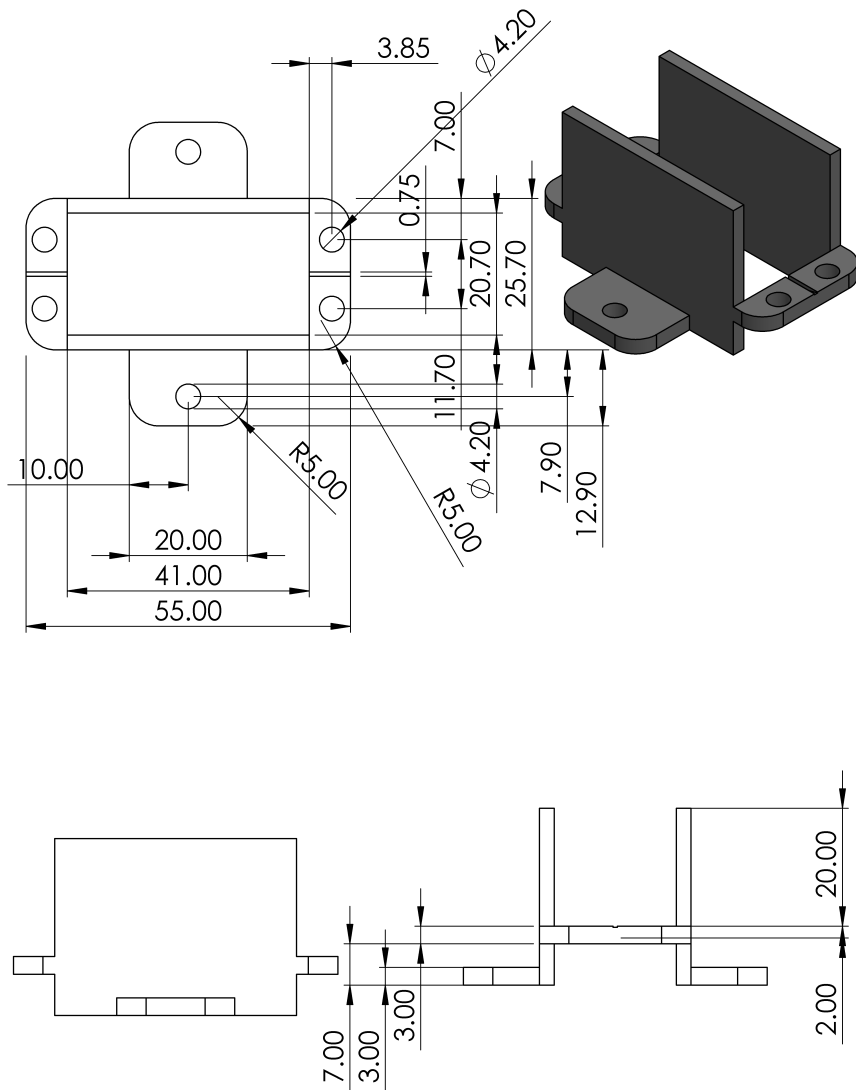


Figure 3.11: Servo motor cage

- **Mounting plate**

Figure 3.12 shows the mounting plate for the motor cage. The plate is like a ring with slots. The design allows for rotation without the need to reposition the supporting rods.

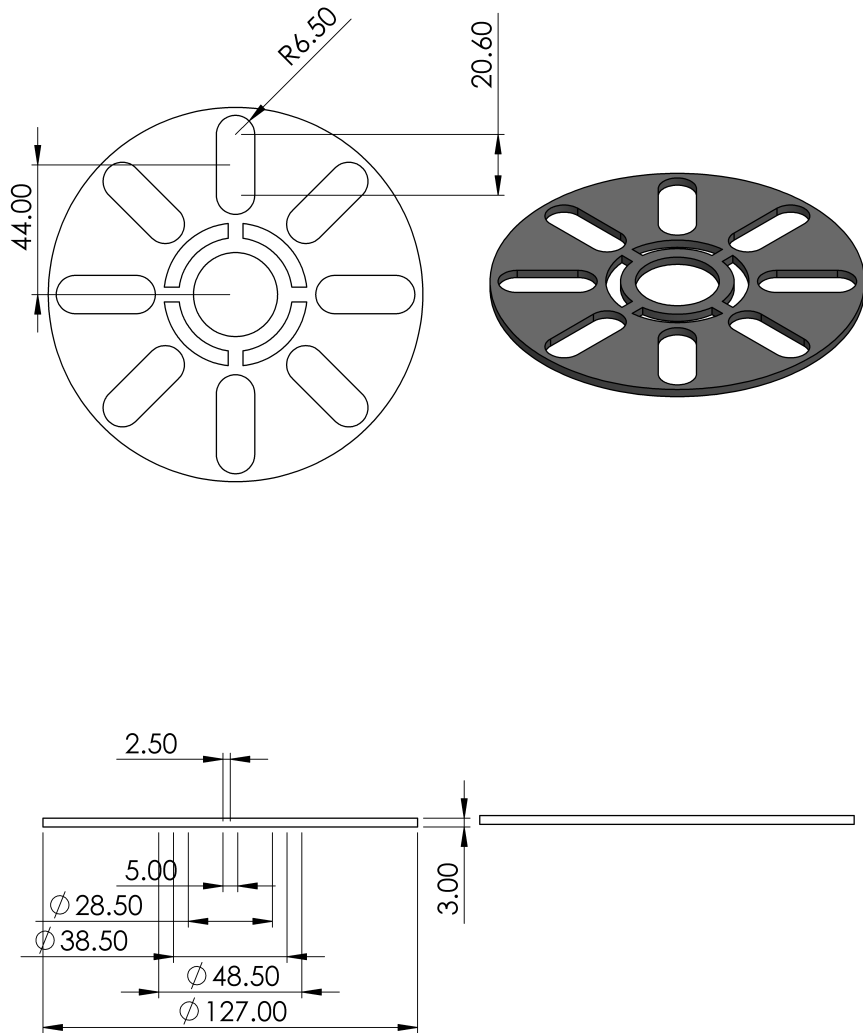


Figure 3.12: Servo motor mounting plate

- **The holder assembly**

Figure 3.13 shows the servo motor cage with the servo motor mounted on the mounting plate. The servo motor assembly can be rotated and translated to reposition the line of rotation of the motor axle.

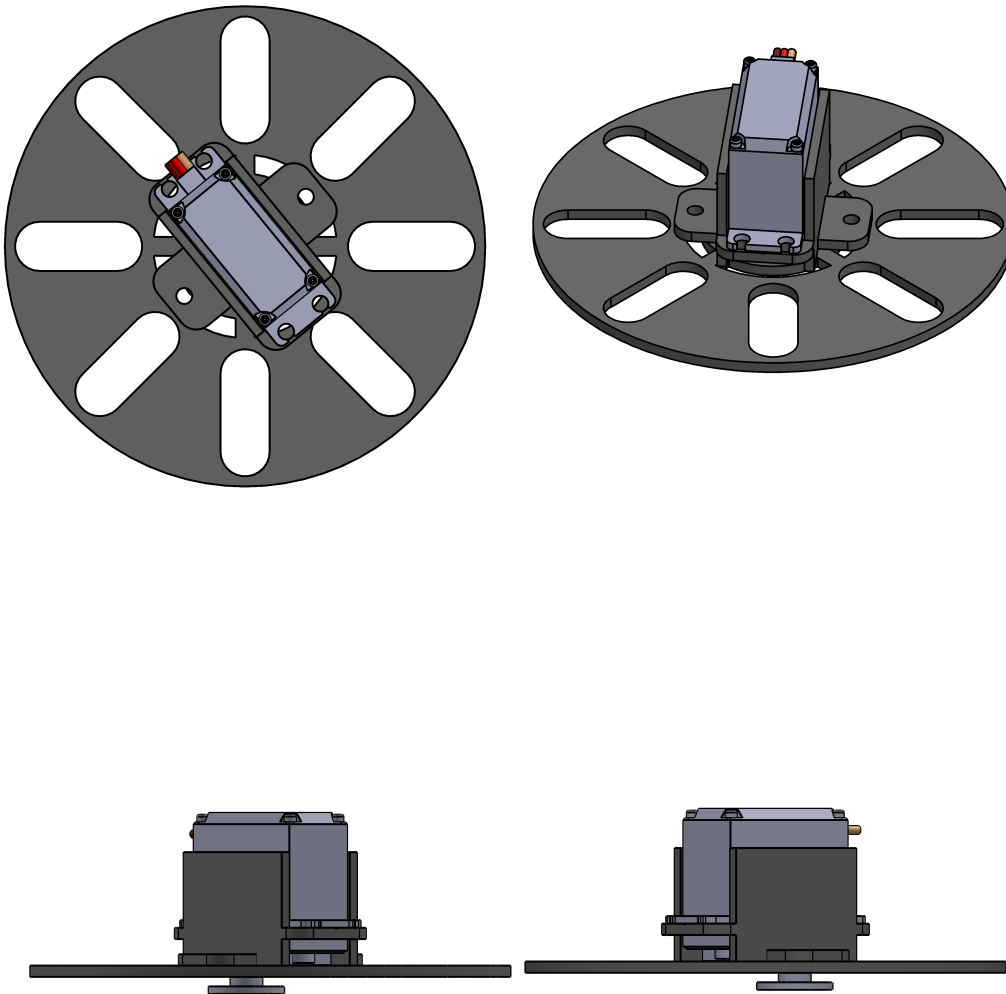


Figure 3.13: Servo motor mounted assembly

This design can allow for both rotational and translational adjustments along the slots. However, it is complex and require a lot of fasteners.

- ii. A combination of spur gears to always translate the line of rotation of the motor axle to a fixed line of rotation no matter the orientation of the motor.

Designs with the spur gears approach

- Spur gears

Spur gear shown in Figure 3.14 translates the line of rotation by 5.75mm in any orientation of the servo to a fixed centre line.

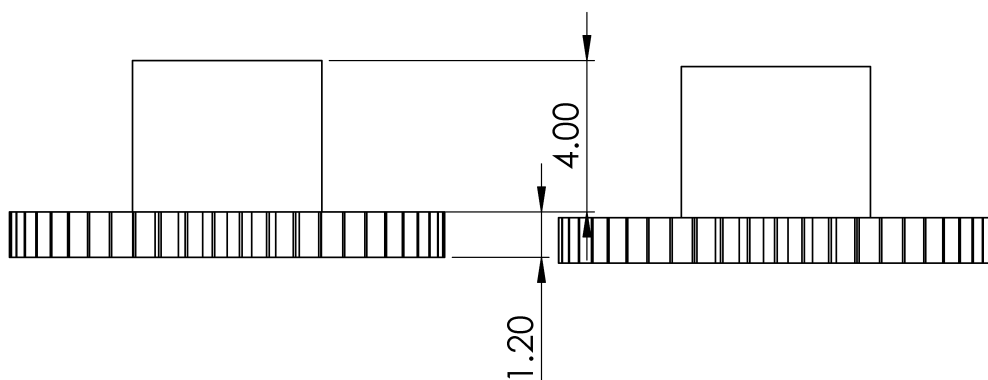
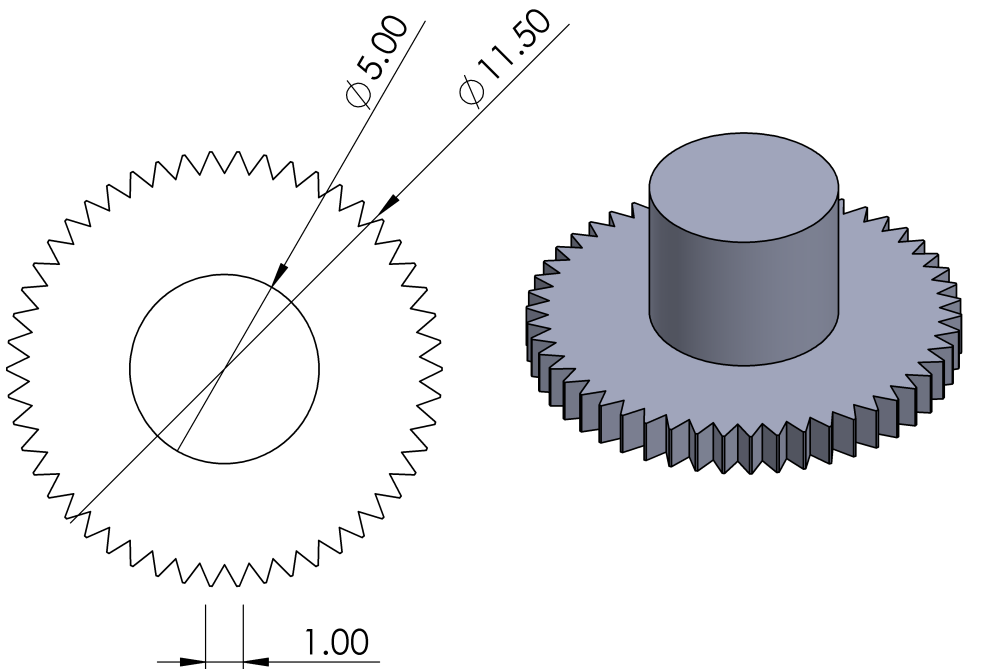


Figure 3.14: Spur gear

- **Servo motor-spur gear assembly**

Figure 3.15 shows the spur gear translation system assembled with the servo motor.

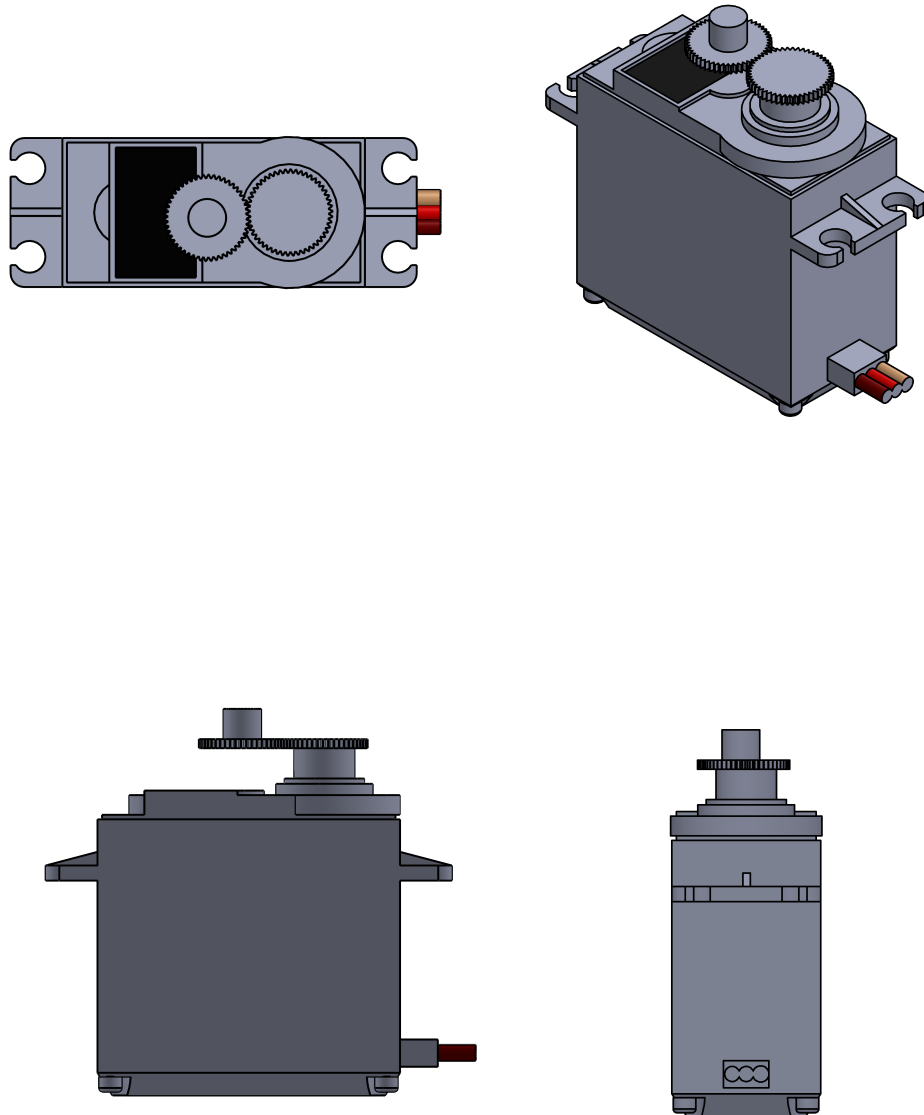


Figure 3.15: Servo motor with spur gears

This design is quite simpler than the first approach. The design considerations are few and can produce even finer translations in the scale of the spur gear pitch(1mm). However, the main challenge with this

design is the durability of spur gears made of PLA material since servo motors then have a high starting torque. This will almost necessitate the replacement of the gears after every two or three experiments.

Between the two mounting designs described, the first options had more merits than the second option. It might require more material to produce it but at least it is only for one time unlike with second option where the gears are to be replaced after every two or three times in operation.

(b) **Mounting rod**

Two of the rod shown in figure 3.16 are used to support the mounted servo motor assembly on the ball valve. The design was such that it allowed for fasteners on both sides: at one end, to fasten the servo motor assembly after alignment and at the other end, to fasten the whole flow control unit on the main discharge pipe.

The protrusion of its surface eliminates the need for another fastener.

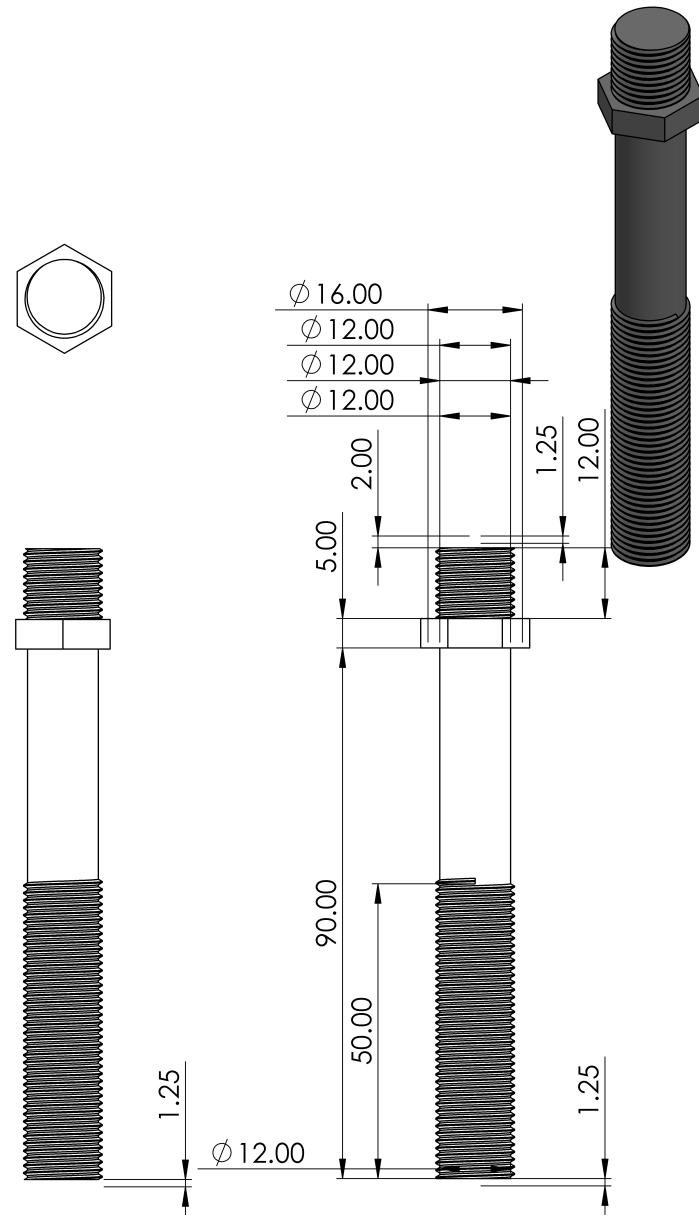


Figure 3.16: Mounting rods

(c) Interface

The interface shown in Figure 3.17 is an improvement from the interface that was used with the stepper motor. This design is minimalist and requires a lesser volume of material to produce. In addition, it also has provisions(hooks)

to allow for even finer adjustments in the first approach for mounting the servo motor.

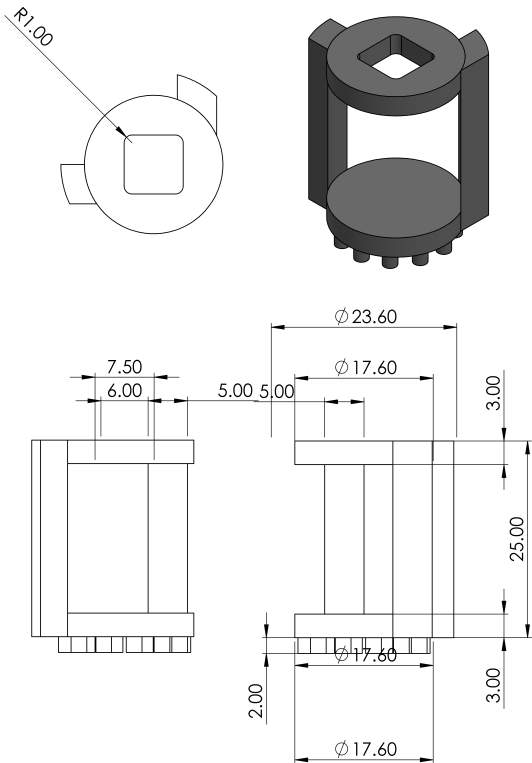


Figure 3.17: Interface

(d) Straps

Serrated straps shown in 3.19 are also an improvement on the straps used in the stepper motor approach. The serration provide more grip on the discharge pipe. It can also support more load.

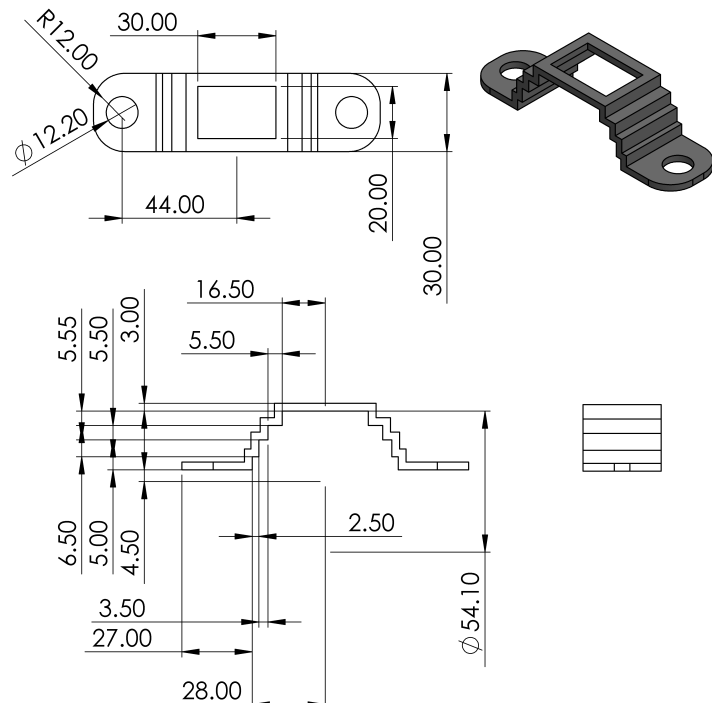


Figure 3.18: Top strap

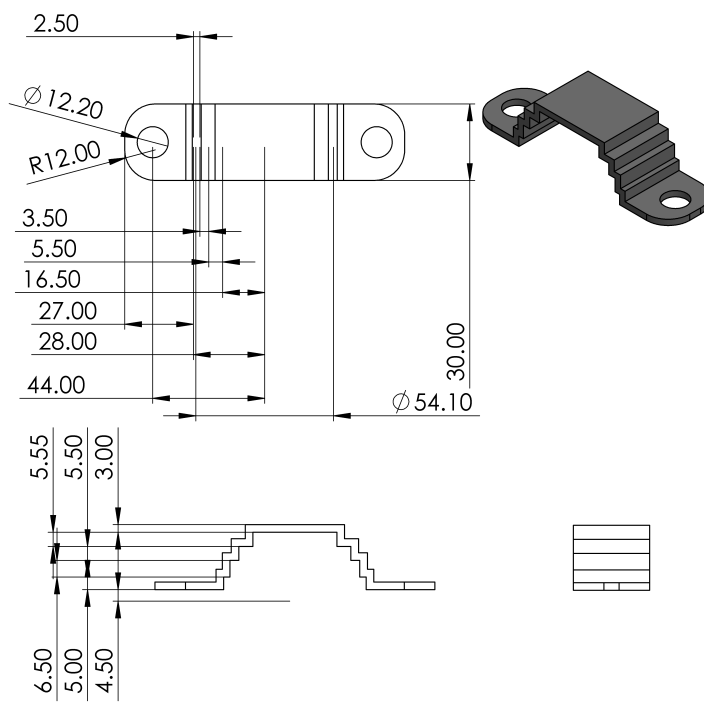


Figure 3.19: Bottom strap

(e) Servo motor discharge flow control assembly

The assembly of parts used in the servo motor approach is as shown in Figure 3.20.

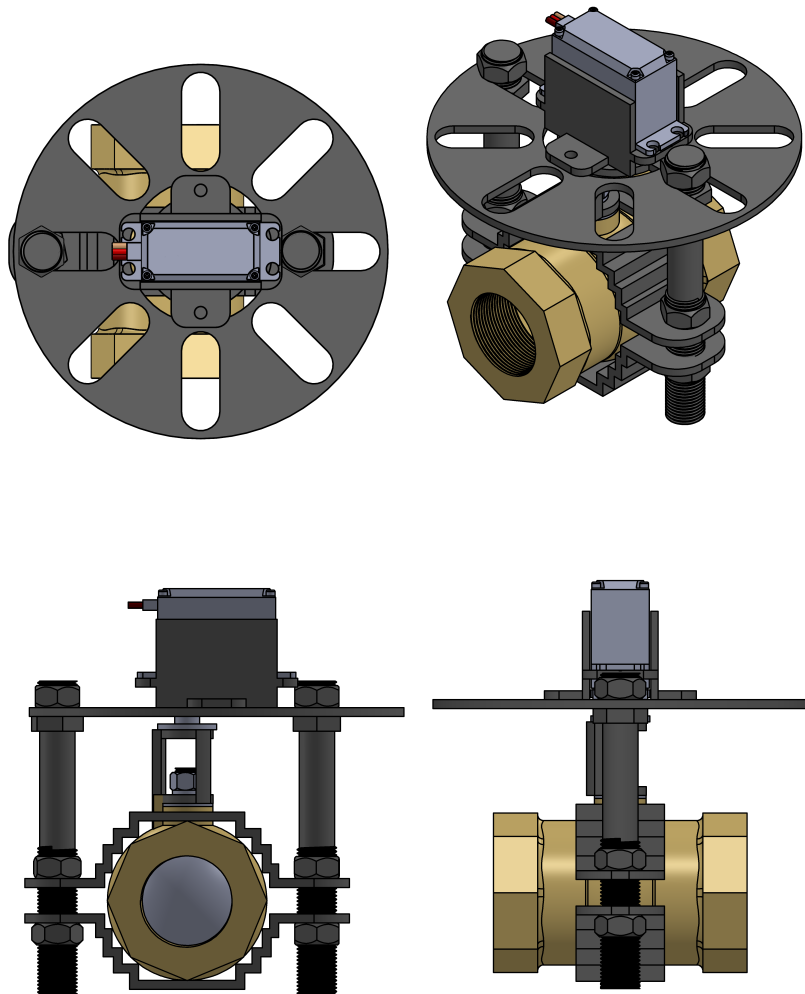


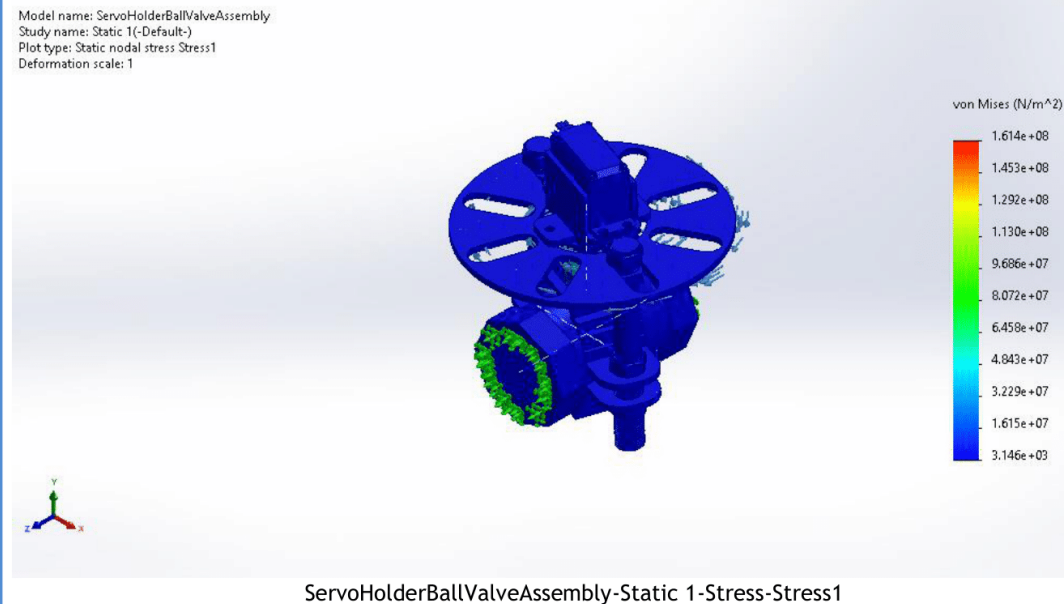
Figure 3.20: Servo motor discharge flow control assembly

(f) Finite element analysis of the assembly

PLA material was assigned to each part of the structure. The maximum load torque of the servo motor($11kg.cm$) was then applied on the mounting plate of the motor. The results of the simulation were as shown in figure 3.21. From the results, the structure still holds to the maximum torque with minimal displacement.

Study Results

Name	Type	Min	Max
Stress1	VON: von Mises Stress	3.146e+03N/m^2 Node: 83976	1.614e+08N/m^2 Node: 7197



Name	Type	Min	Max
Displacement1	URES: Resultant Displacement	0.000e+00mm Node: 15478	2.644e+01mm Node: 109181

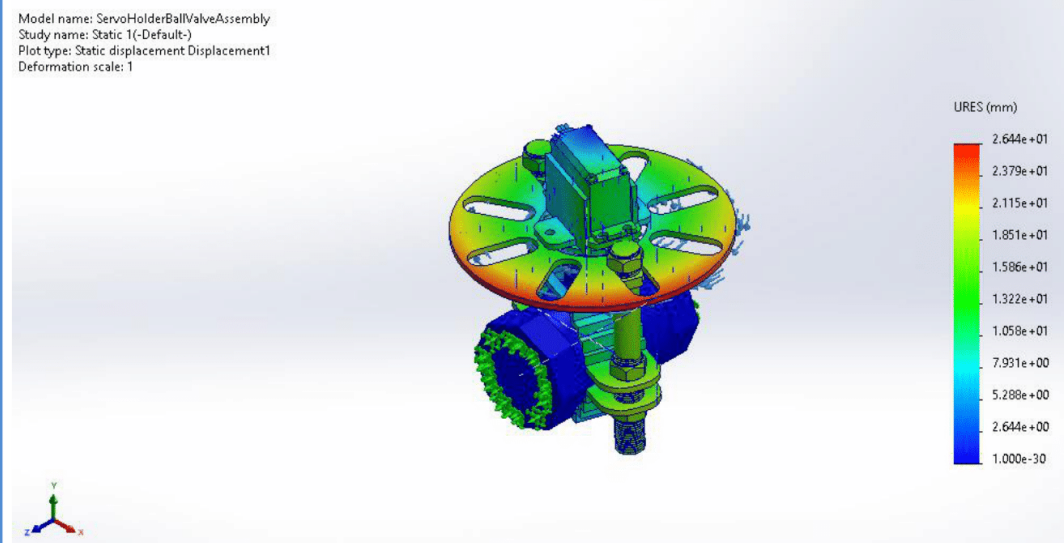


Figure 3.21: Servo Assembly simulation results

From these two design approaches, the servo motor approach was selected.

3.2.2 Flow diversion sub-unit

The design of this unit was based on the following two considerations:

1. A faster response time. The response time in this application is the time it takes to divert the discharge flow into the main reservoir or the discharge collection tank.
2. An actuator that can provide linear translation of not less than 30 mm. In fact the longer the better. This is measured from the design assembly. This ensures that the discharge is fully diverted into the collection tank or to the main reservoir.

Based on the above two considerations, the following two design options were feasible.

1. Piezo-electric actuator

Piezoelectric actuators are transducers that convert electrical energy into a mechanical displacement or stress based on a piezoelectric effect, or vice versa. They are widely used as a high-precision positioning mechanism since they can control a small mechanical displacement at high speed, with the advantages of large generated force, stable displacement, and ease of use [15].

Among the many advanced piezoelectric actuators on the market, a Xeryon Precision XLA-Series 3 piezo actuator shown in Figure 3.22 was selected since it satisfied all the design requirements required for this subunit.

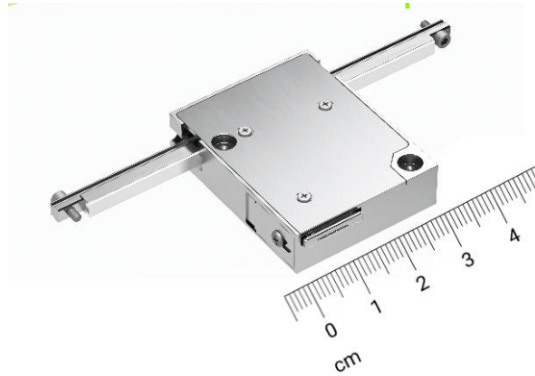


Figure 3.22: Xeryon-XLA Series 3 piezo actuator [16]

Its technical specifications are as shown in table 3.3.

Property	Value
Stroke Length	45mm
Resolution	312nm
Operating voltage	20-48V
Control	Closed loop control with an external XD-A controller
Temperature	-30 to 70
Holding& Driving force	3N
Speed range	2mm / s to 400mm / s

Table 3.3: XLA series 3 piezo actuator specifications [16]

From the technical specifications in the table, it is evident that this actuator could be the best choice for this application. However, it requires an external proprietary controller for closed-loop control. Xeryon company products are also not available in public stores such as Amazon or Aliexpress.

2. Electromagnetic Actuator

Electromagnetic actuators work on the principle of electromagnetism. Electrical energy is converted to a linear translational mechanical motion and vice versa. The

electric current serves as the actuator quantity in electromagnetic actuators.

Based on the design considerations, a P16-S micro linear actuator shown in figure 3.23 was selected for this application.



Figure 3.23: P16S linear actuator [17]

Its technical specifications are shown in table 3.4.

Property	Value
Operating voltage	12V DC
Stroke length	100mm
Stroke speed	150mm/s
Maximum load	6.4N

Table 3.4: P16-S Micro-linear actuator technical specifications [17]

From the technical specifications in the table, it is also evident that this actuator satisfies optimumly the requirements required for this application. Unlike the piezo actuator, this device is available for less than \$ 35 in e-Commerce stores such as Amazon or AliExpress.

Based on the above descriptions, the P16-S micro-linear actuator was selected for this application mainly because of its availability.

In order to hold this actuator in position the following designs were made:

1. Electromagnetic Actuator holder

This unit supports the actuator on the ball valve. It is required that this unit will withstand the weight of both the actuator and the diverter. Its design is as shown in figure 3.24.

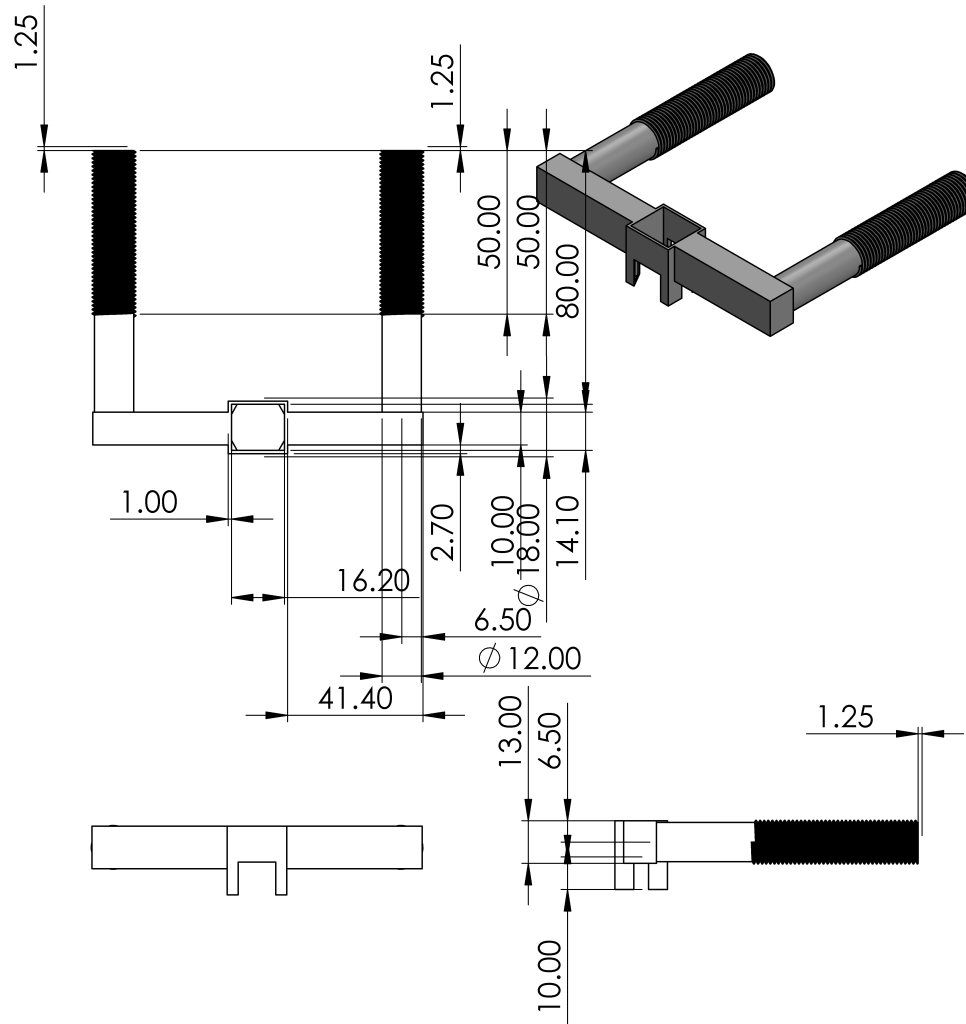


Figure 3.24: Electromagnetic actuator holder

The dimensions of this holder design were determined from the dimensions of the P16-S linear actuator plus a clearance of 0.5mm.

2. Diversion Flap

In order to divert the flow, a channel-like flap is to be used. The design of the flap is as shown in figure 3.25.

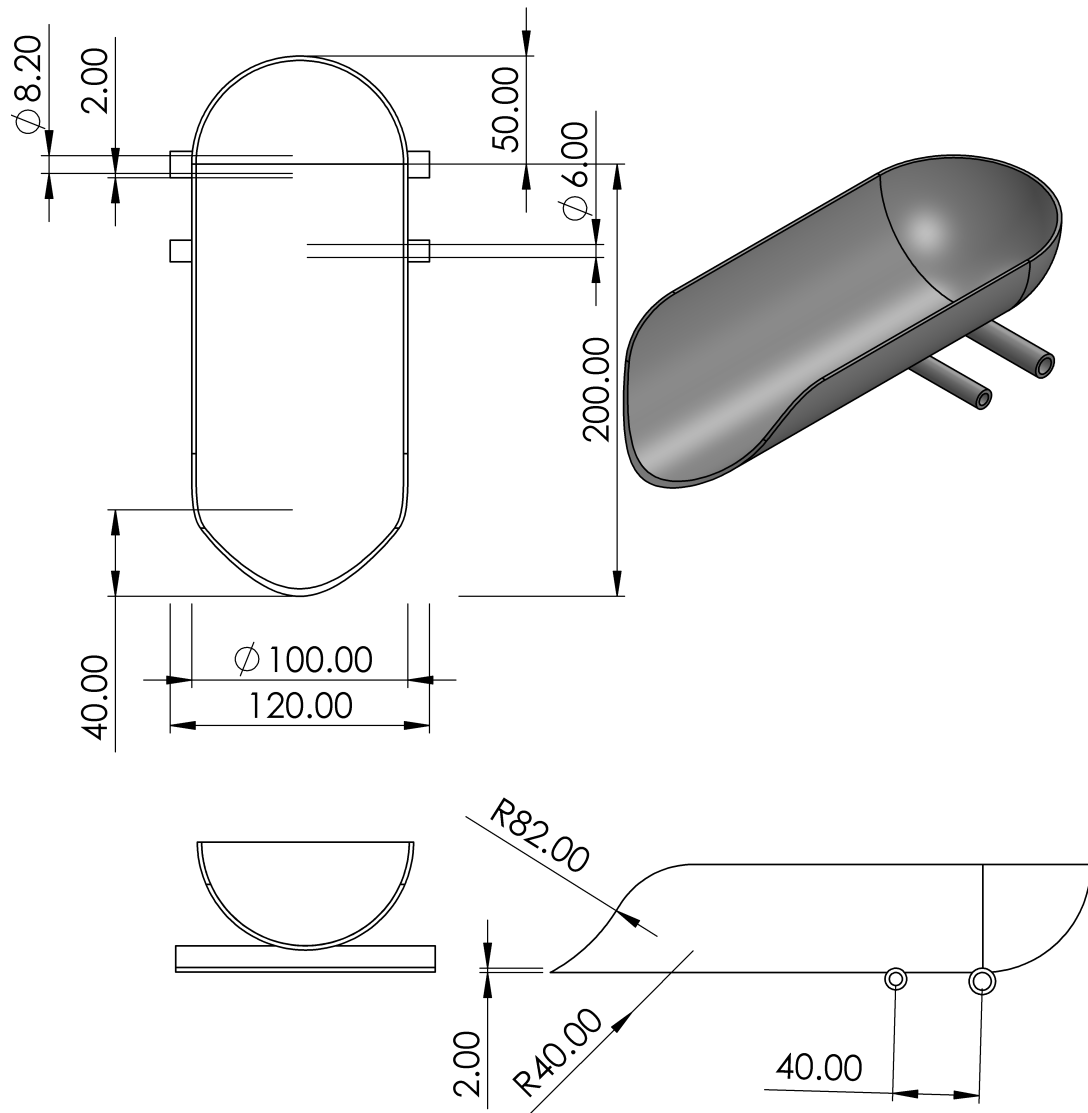


Figure 3.25: Diversion flap

The design was such that it can tap the whole stream from the $1\frac{3}{4}$ inch main discharge pipe on the main machine. Its 150mm length is determined by the length of the gap between the discharge pipe and the collection unit.

3. Flap support frame

This structure supports the diversion flap in place below the discharge pipe. This design was necessary since there is no convenient mounting point on the main machine that can allow the flap to be mounted without making changes to the main machine. Its design is as shown in figure 3.26.

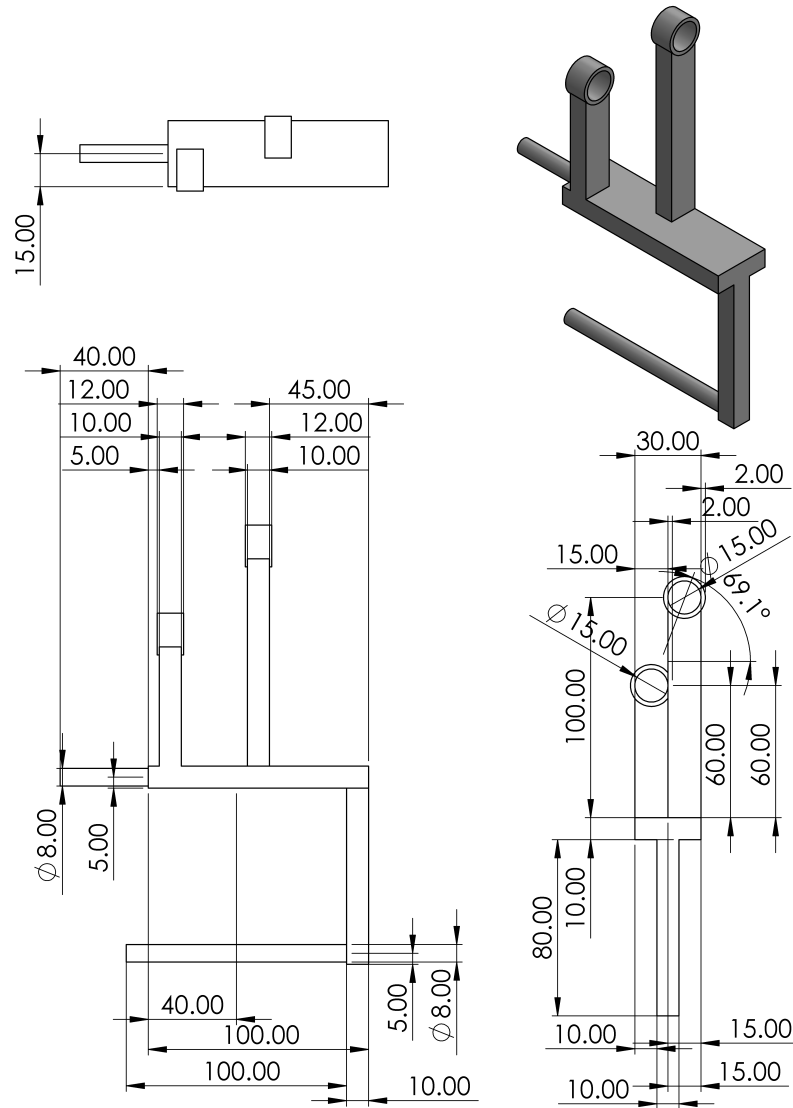


Figure 3.26: Flap support frame

This frame also provides an extension for supporting the kinematic chain that flexes

the flap.

4. Kinematic Chain

To amplify the 100mm translation in order to flex the flap enough, a four-bar kinematic mechanism is used. The lengths of the links and the orientation of the four bars are determined by assuming a translation of 100mm at the output.

Using the MechDesigner software, the kinematic chain is designed to provide the required motion for the flap. The CAM data from its simulation are exported automatically to a SolidWorks model of the fixed point of the part.

(a) Crank

The input translation from the linear electromagnetic actuator. The design of this link is as shown in figure 3.27.

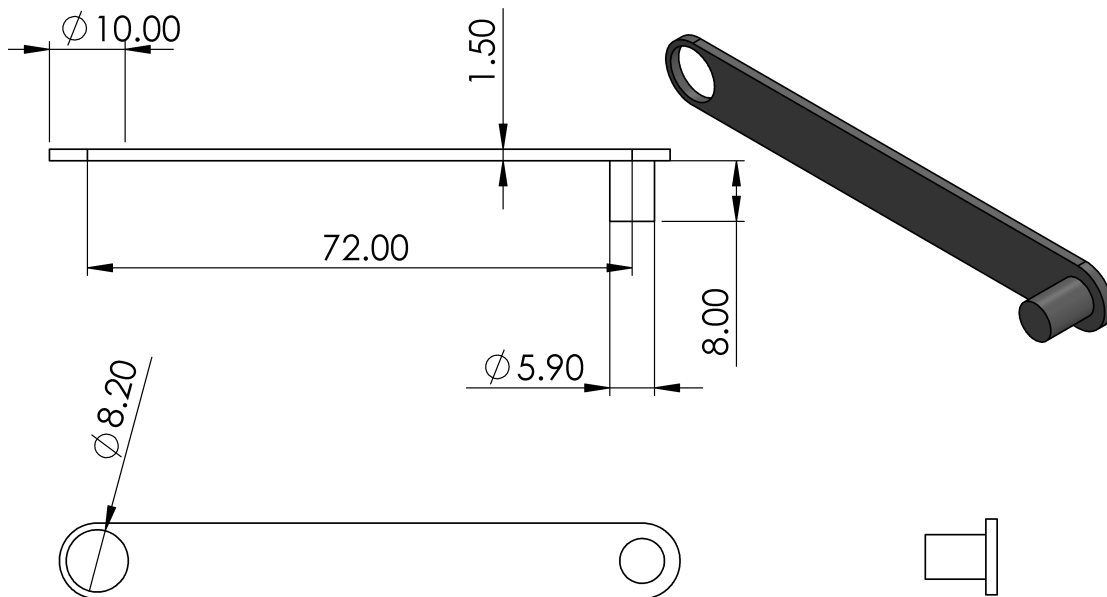


Figure 3.27: Crank

The connection between this link, the end of the actuators and the couple is a series of joints. The translation is in two axes: X and Y axes.

(b) Coupler

This link transfers the motion to the output link: the rocker. Its design is shown in Figure 3.28.

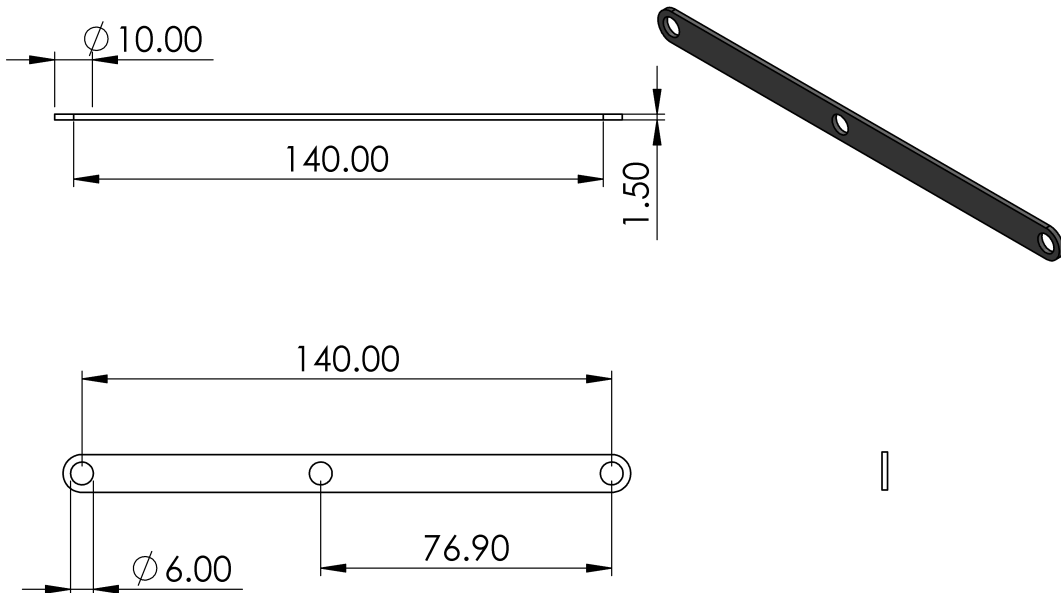


Figure 3.28: Coupler

The design is such that it hinges on an extension from the flap support frame on one end and connects to the rocker on the other end. The crank is connected at a distance from one end.

(c) Rocker

The rocker connects to the coupler on one end and to the flap on the other end. Its design is as shown in figure 3.29.

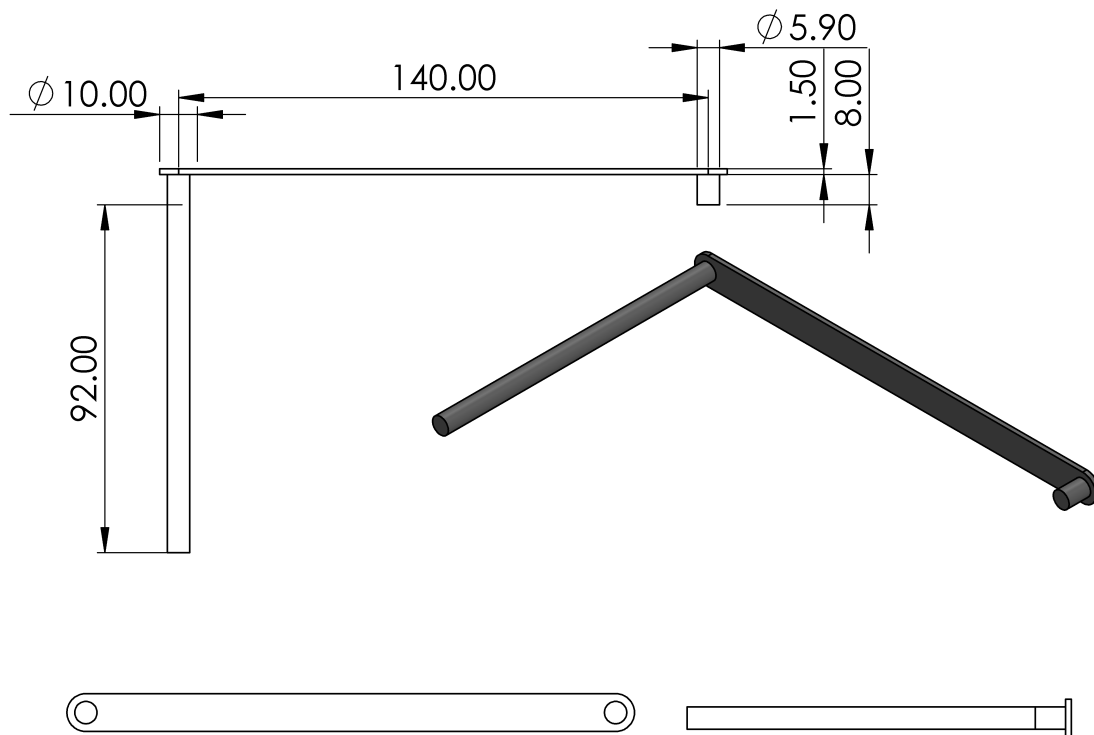


Figure 3.29: Rocker

5. Discharge flow control sub-unit

In the assembly shown in Figure 3.30, the flap support frame hinges on two rods: one of the servo mount rods and the other is one of the legs of the electromagnetic holder.

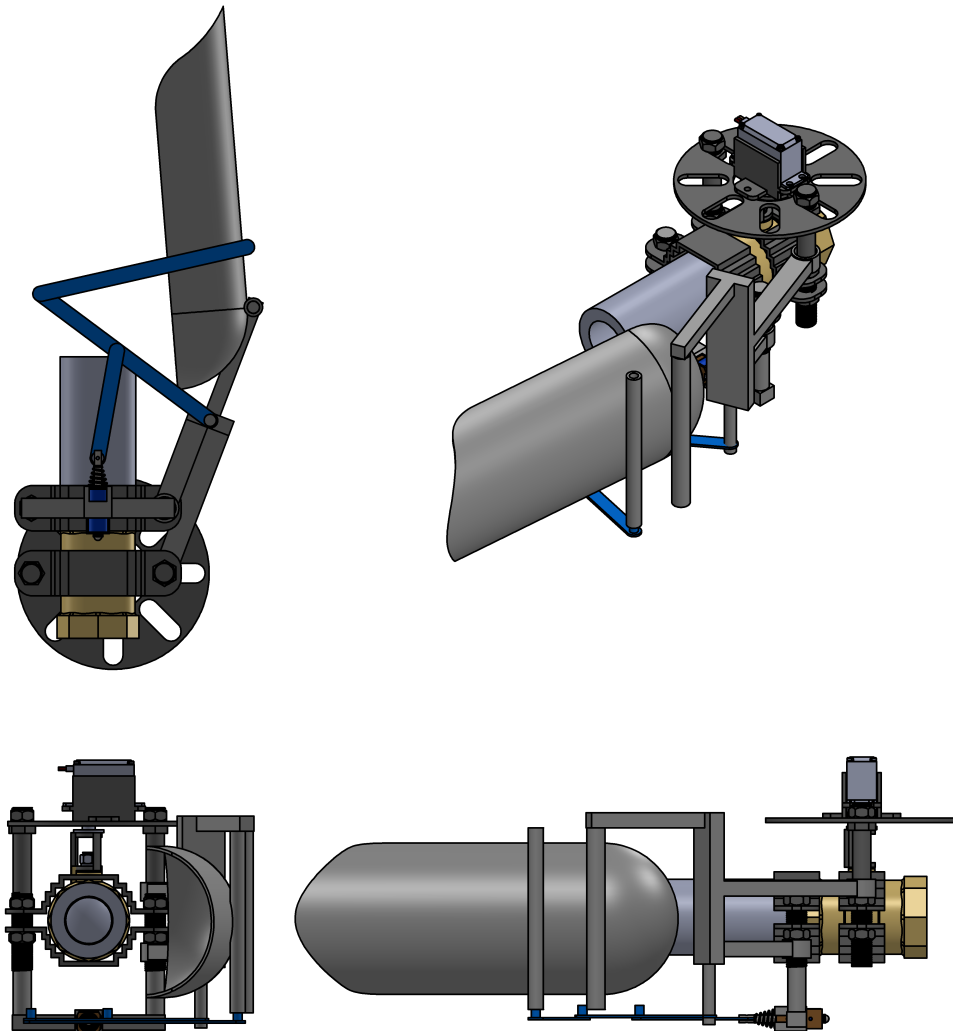
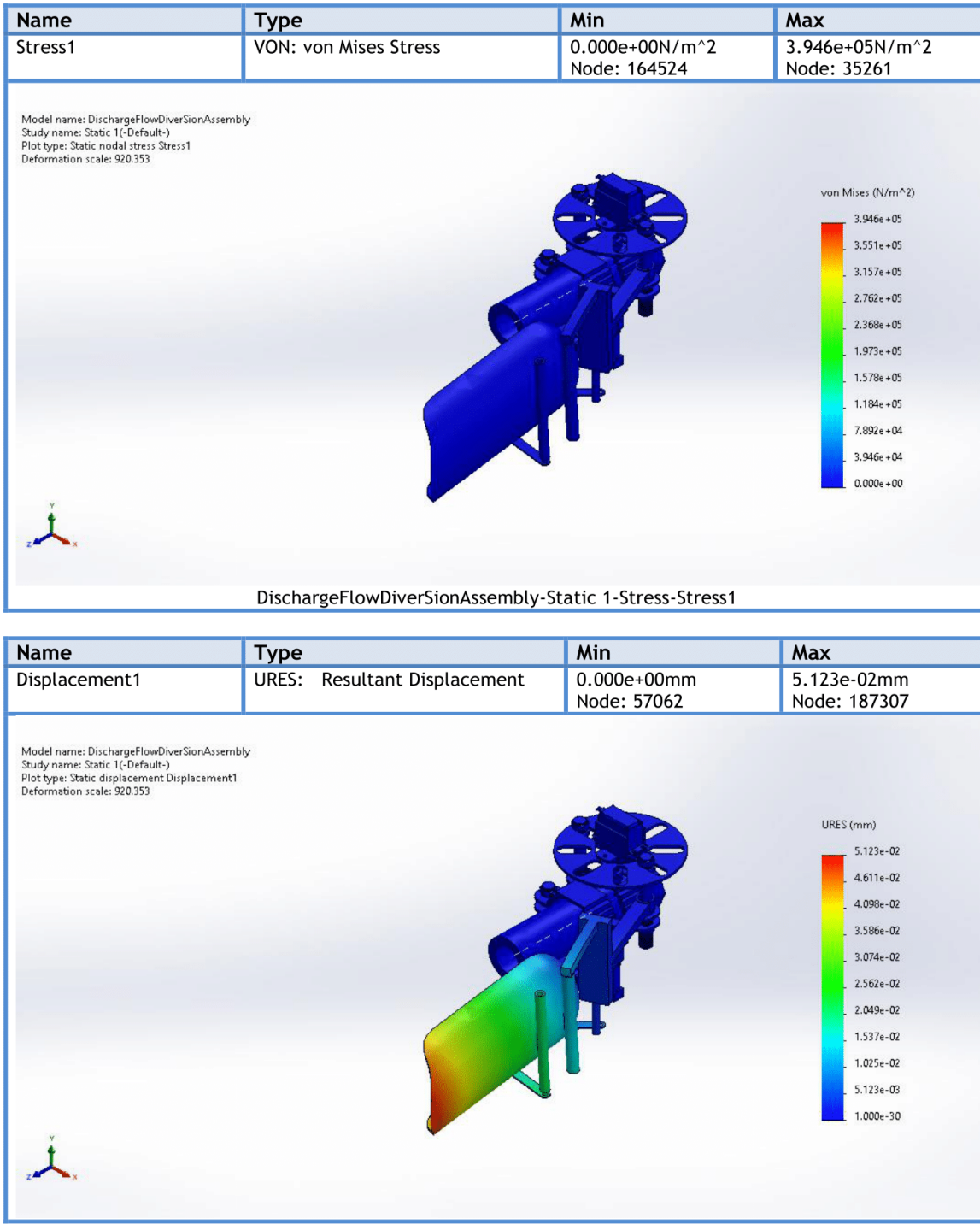


Figure 3.30: Flow Diversion assembly

6. Finite element analysis of the electromagnetic actuator assembly

The finite element analysis of the assembly was performed to test how the electromagnetic diversion system is stable under a pressure force of $1N/m^2$ applied to the inside of the flap. The results of the simulation are shown in figure 3.31.

Study Results



SOLIDWORKS

Analyzed with SOLIDWORKS Simulation

Simulation of DischargeFlowDiverSionAssembly

17

Figure 3.31: Diversion assembly FEA results

From the results in figure 3.31, it is evident that the electromagnetic actuator assembly holds up to the amount of distributed pressure on the flap.

3.2.3 Electrical

1. MG996R Servo motor connection

- **Power requirements**

From the technical specifications of the motor listed in table 3.2, this motor's operating voltage is 4.8V-7V, its driving current is between 500mA and 900mA, and its stall current is 2.5A(6V). However, most microcontrollers supply up to +5V DC voltage. This therefore requires a step-up circuitry or an external voltage supply to the motor.

- **Connection**

To connect an external supply requires a circuit shown in figure 3.32.

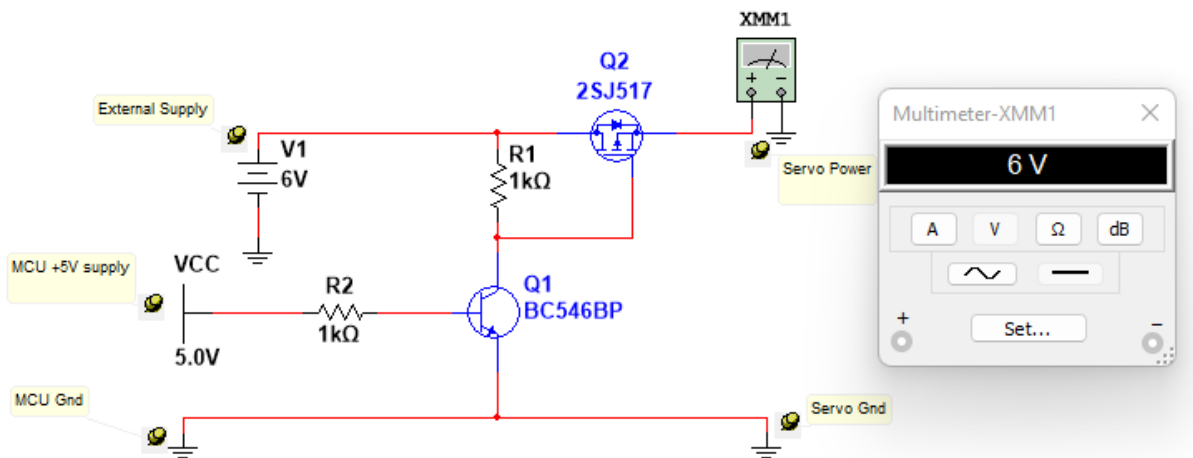


Figure 3.32: Servo Connection

A 6V DC external supply is connected to the drain terminal of a Power MOSFET. This is activated by an NPN BJT transistor using the voltage supplied by the microcontroller.

2. P16-S Electromagnetic Actuator connection

- **Power requirement**

The power requirements for this actuator are 12V DC supply and 2A current as listed in table 3.4. These two power requirements cannot be satisfied by just a micro-controller; an external source is necessary.

- **Connection**

This two power requirement can be satisfied using a combination of a MOSFET power IRF520 and a D1 flyback diode as shown in Figure 3.33.

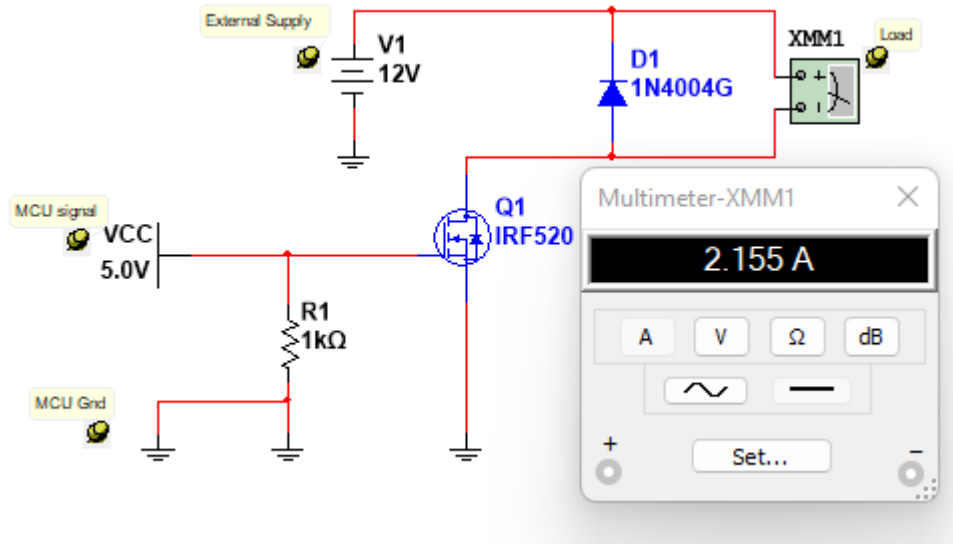


Figure 3.33: Electromagnetic Actuator circuit

This is available in a module shown in figure 3.34.



Figure 3.34: IRF520 Module [18]

3.2.4 Software and control

1. MG996R Servo motor control

- Requirements

This motor is required to drive the ball valve in steps in a 90^0 turn, the angle covered to close and open the ball valve. However, the motor can turn 120^0 . Therefore, the 90^0 turn can be achieved by Pulse Width Modulation.

- Control

From the motor's datasheet, the period of the motor's control signal is 50Hz(20ms). This is checked against the clock frequency of the microcontroller and used to determine the prescaler value for the timer register.

For example:

Consider a micro-controller with clock frequency: $84MHz$

$$\text{Timer_Frequency} = \text{Period} \times \text{PWM_Frequency}$$

$$\therefore = 20000 \times 50Hz = 1MHz$$

$$\text{Pre_scaler} = \frac{\text{Clock_frequency}}{\text{Timer_frequency}}$$

$$\therefore = \frac{84}{1} = 84$$

The angle turned by the motor is proportional to the Logic HIGH duty. Therefore, by writing a time value for 90^0 full turn in the timer register, the turn can be achieved. Smaller turns can be achieved by writing corresponding time values to the timer register.

2. P16-S electromagnetic Actuator control

- **Requirements**

In order to divert the flow, this actuator is required to provide a linear stroke and remain in position for a set amount of time. When the time elapse, it is required to linearly retract in order to restore the flow.

- **Control**

This actuator provides a full length stroke in;

$$\text{Full length of a stroke: } = 100\text{mm}$$

$$\text{Stroke_speed} = 150\text{mm/s}$$

\therefore Time taken for a full length stroke is $\frac{10}{15}^{th}$ of a second.

This is achieved when it is powered. The terminals are switched in order to retract it.

Shorter strokes can be achieved by turning on the actuator for a time less than $\frac{10}{15}^{th}$ seconds.

Controlling these two electronics requires an RTOS platform. There are many RTOS platforms but Zephyr and Mbed platforms are preferred because of their relatively large support with extensive APIs.

3.3 Discharge Handling Unit

This unit consists of the following subunits:

1. Discharge collection tank sub-unit.
2. Outlet valve sub-unit.
3. Weight measurement sub-unit.
4. Temperature measurement sub-unit.

3.3.1 Discharge collection tank sub-unit

- **Collection tank**

This is used to temporarily collect the discharge from the pipeline during each step of an experiment, after which it is released to the main reservoir through an outlet valve0. The weight and temperature of the discharge are also taken in this tank.

The following design considerations were made when selecting a tank for this application.

1. Shape of the tank

The design of this tank should be such that the tank discharges in the least time possible with no remnants. Therefore, the shape of the tank was put into much consideration such that it influences/motivates the discharge. This consideration was made in tandem with the consideration of the position of the outlet valve.

2. Material of the tank

The collection tank will hold water with chlorine chemicals. This brings about the thread of rust. Therefore, the tank material was chosen so that it minimises this thread.

3. Volume of the tank

The volume of the tank was such that it can hold a stream from the $1\frac{3}{4}$ inch main discharge pipe that flows for approximately 30 seconds when the valve is fully opened. This was around $0.01m^3$. Therefore, the dimensions of the tank were such that it produced a volume of this value.

Based on the above considerations, two options were technically feasible in terms of the available means for fabrication:

1. Cuboid tank

The design of the tank is shown in Figure 3.35.

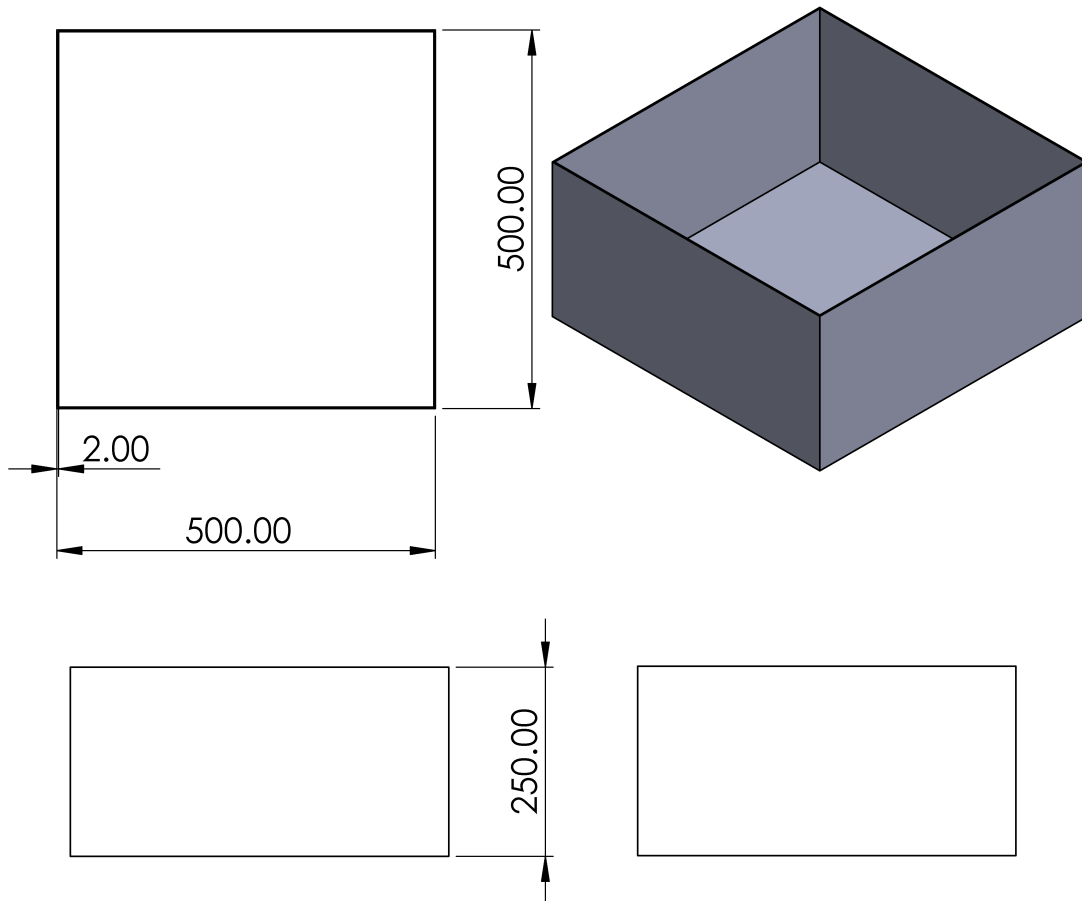


Figure 3.35: Cuboid discharge container

This tank satisfies the requirements for this application. However, a small volume of discharge will tend to remain in the tank when the tank is emptied.

2. Horizontal Cylindrical tank

The design of this tank is shown in Figure 3.36.

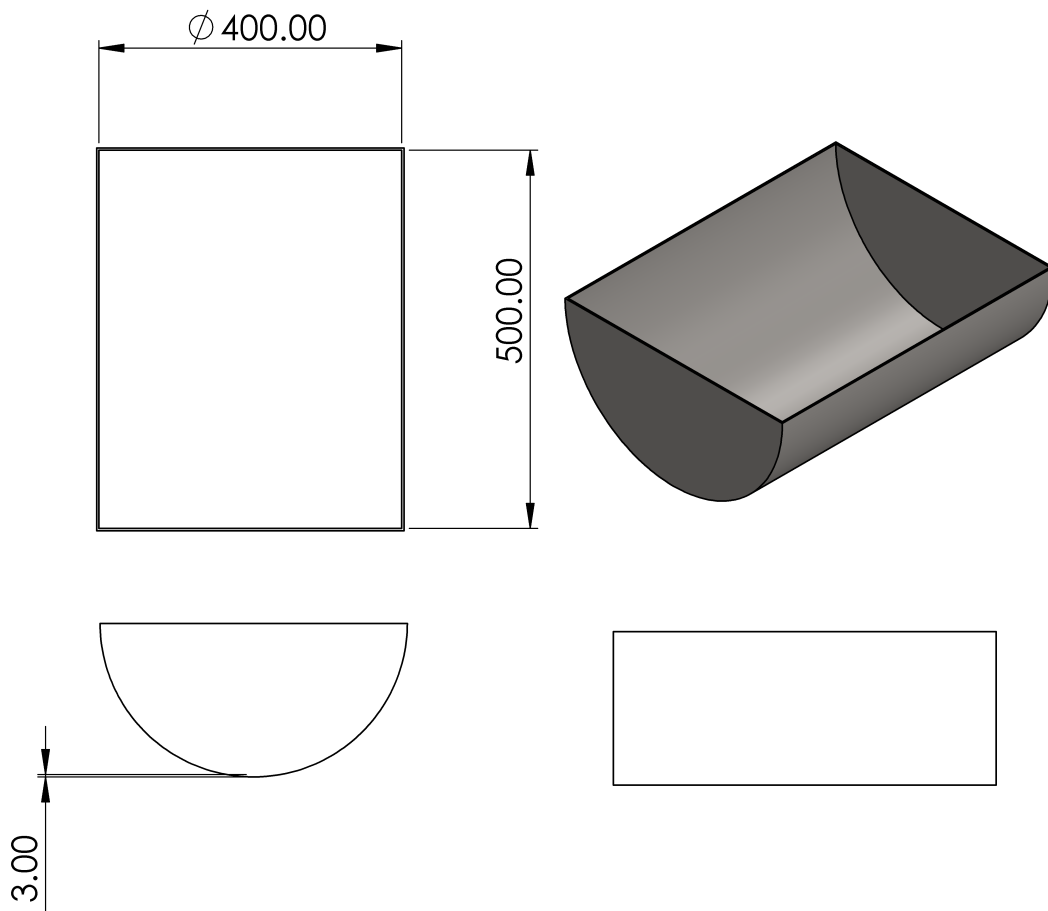
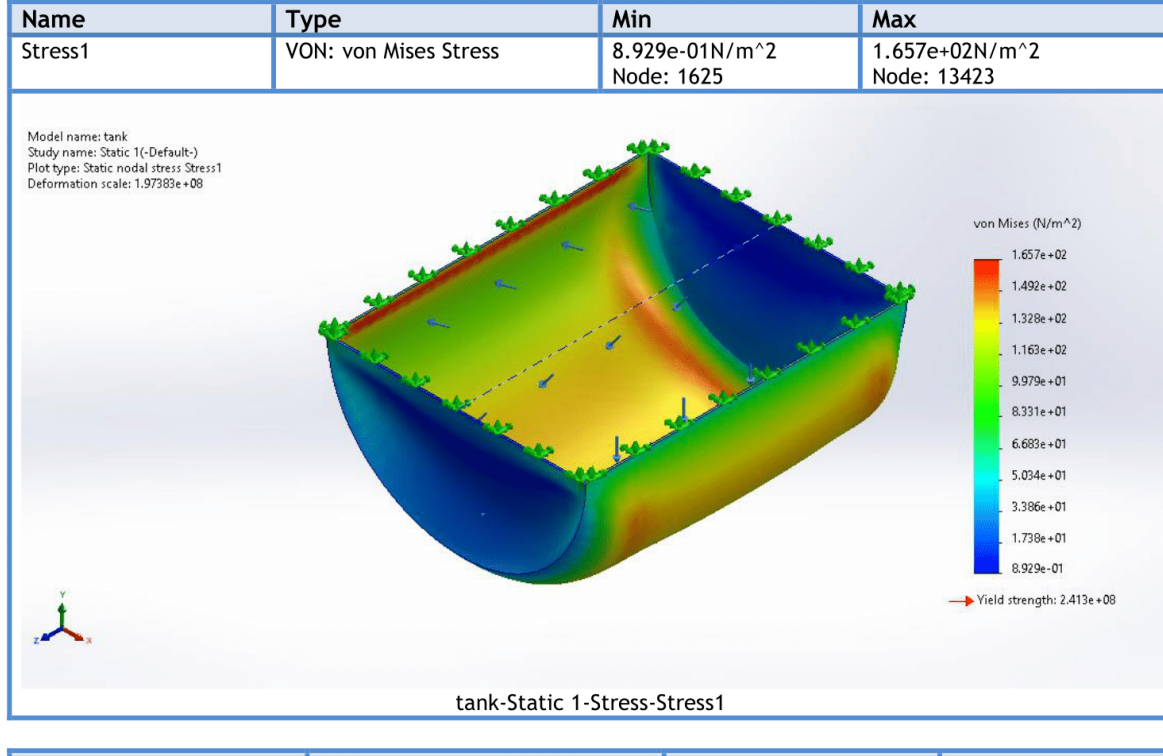


Figure 3.36: Horizontal Cylindrical tank

When emptying this tank, the tank motivates the flow out of the discharge due to the concentration of the pressure of the discharge on a line at the bottom of the container, as shown by the results of the study simulation in Figure 3.37.

Study Results



Name	Type	Min	Max
Displacement1	URES: Resultant Displacement	0.000e+00mm Node: 1	2.564e-07mm Node: 10965

Figure 3.37: Tank simulation results

The horizontal cylindrical tank was selected for this application.

- **Tank support frame**

In order to support the tank in an upright position on a flat surface a support frame shown in figure 3.38.

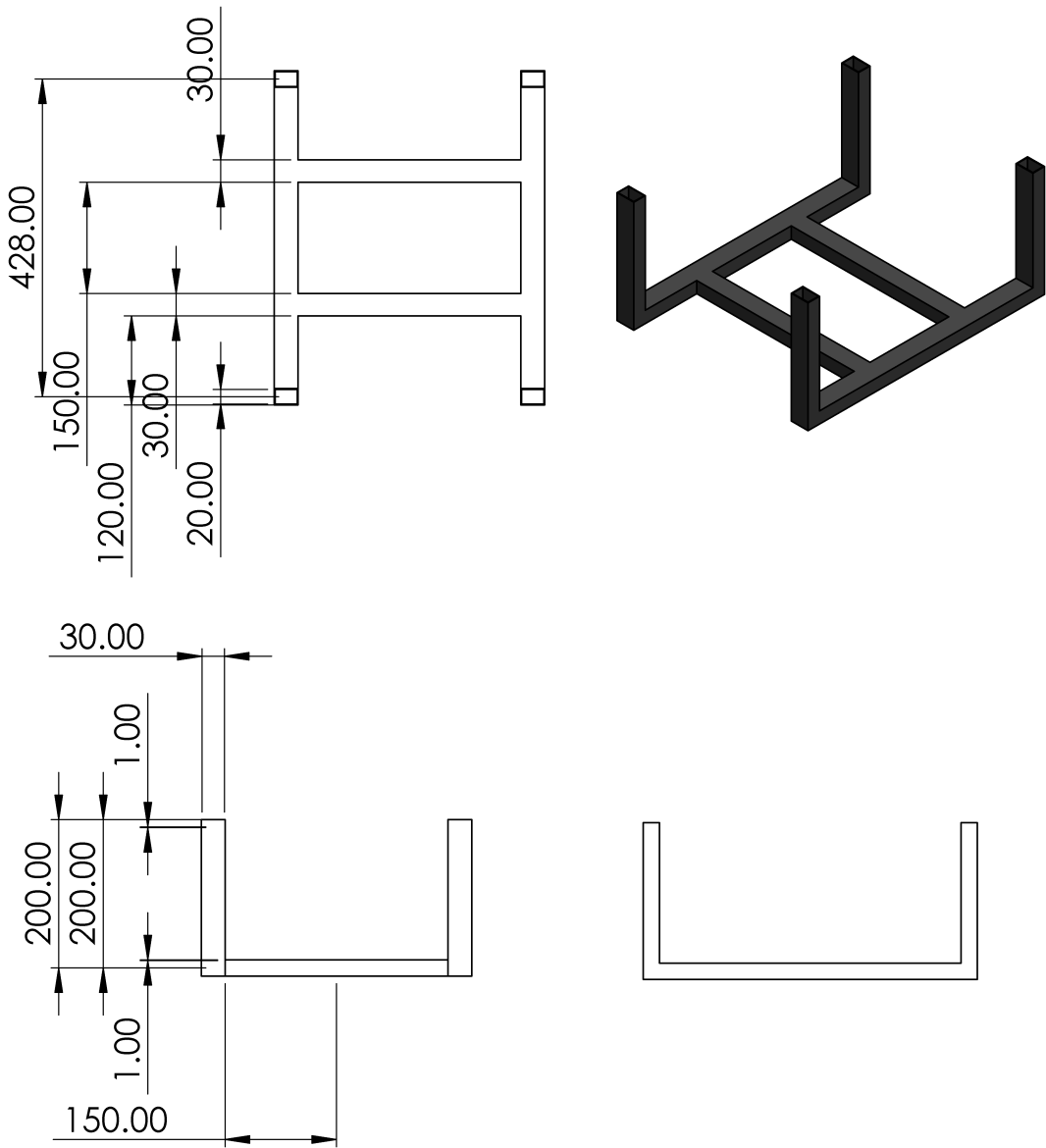


Figure 3.38: Cylindrical tank support frame

The dimensions of the frame were such that it provides a clearance of 1mm for the tank.

- **Tank assembly**

The assembly of the tank and its support frame are as shown in figure 3.39.

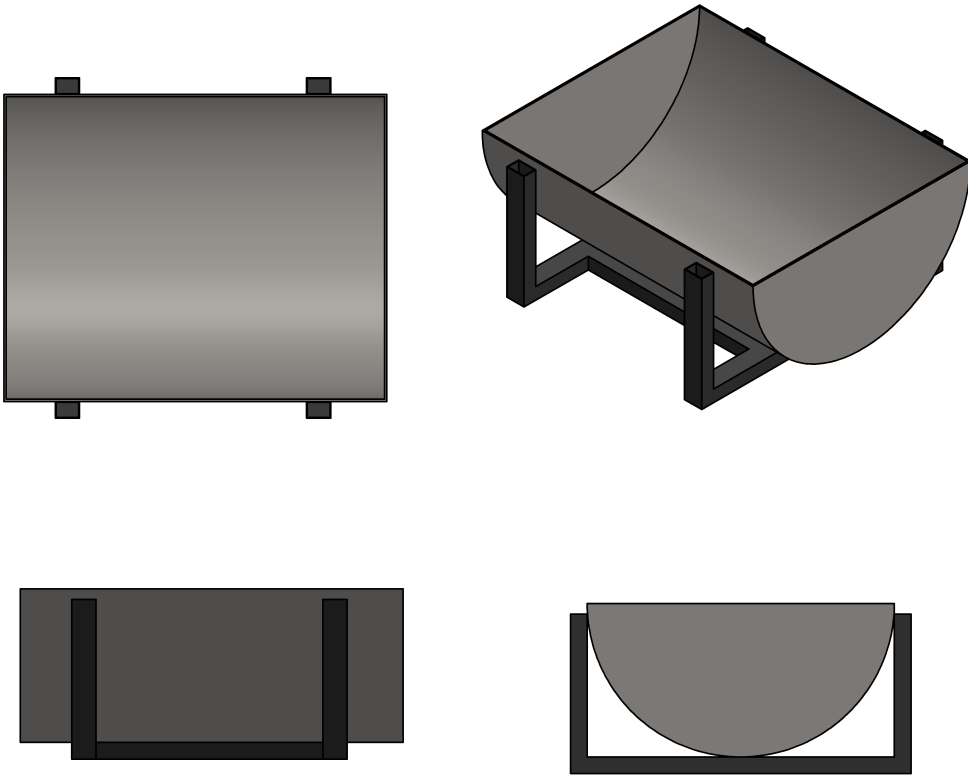


Figure 3.39: Collection tank

- **Position**

The positioning of the tank was also a critical aspect of the design. Ideally, the collection tank was to be either positioned directly just below the flow diversion unit or at the periphery of the main reservoir. Positioning the collection tank directly below the flow diversion unit mitigates the need for additional components such as diverting pipes. This simply implies that the collection tank would just be provided with a holding mechanism for support upon which it is fitted with a solenoid outlet valve directly into the reservoir. On the contrary, positioning the collection tank on the periphery introduces the need for additional components. This includes a pump system to pump the discharge back into the reservoir, which adds to the overall cost of the project. Positioning the collection tank below the diversion unit was the

feasible option.

3.3.2 Outlet valve sub-unit

This valve is attached to the collection tank and is used to empty the tank into the main reservoir. The main consideration was the response time(time taken to close and open the valve) in the selection of a valve suitable for this application. The following options were feasible:

1. **An electrically Controlled Butterfly valve**



Figure 3.40: Butterfly valve [19]

The operating voltage of the valve shown in figure 3.40 is in the range 12V DC - 230V AC. Therefore, its response time can be reduced by increasing the voltage supply to the solenoid.

2. **A solenoid gate valve(with a plunger)**



Figure 3.41: Solenoid valve [20]

The $\frac{3}{4}$ inch solenoid valve shown in figure 3.41 uses a plunger with a cork for control the flow. How fast the plunger closes the aperture depends on the voltage supplied to the solenoid. The operating voltage of this type of valve is 12V DC.

The solenoid gate valve(with a plunger) was selected for this application mainly because the butterfly valve is expensive relative to the budget set for the project.

3.3.3 Weight measurement sub-unit

The weight of the collected discharge is measured in every step in an experiment done on this machine. The weight can be cumulative or measured per step. In the event of an error, the error is not propagated in the cumulative approach, but it will definitely be propagated to every measurement in the weight-per-step approach. Therefore, the weight-per-step approach was selected for this application.

During the selection of a method to use for weight measurement of the discharge, the following considerations were made:

1. The maximum weight that can be precisely measured by the unit. The maximum weight of the structure to be measured is determined as follows:

Assume the maximum volume of the water collected = $0.01m^3$.

$$\text{Mass}(M) = \text{Density}(\rho) \times \text{Volume}(V)$$

$$\text{Water density}(\rho_{water}) = 1000kg/m^3$$

$$\begin{aligned}\therefore \text{Mass of water}(M_{water}) &= \rho_{water} \times \text{Volume of water}(V_{water}) \\ &= 0.01m^3 \times 1000kg/m^3 \\ &= 10Kg\end{aligned}$$

The measuring device should therefore handle weights of more than 10Kg.

2. The resolution of the device.
3. The credibility of the weight measurement device.

On the basis of the above considerations, the following options were considered:

1. Weight measurement by ultrasonic waves

Ultrasonic waves can be used to determine the depth of discharge in the tank. An ultrasonic wave generator generates an ultrasonic wave and is propagated to the surface of the water. It is then reflected due to refraction to a receiver. The time taken to send and receive the echo is multiplied by the speed of sound to obtain the depth of the empty side of the container.

This approach is rudimentary and very much flawed as there are many considerations in order to obtain almost accurate results. Some of the considerations include:

- (a) The angle of reflexion δ is shown in figure 3.42.

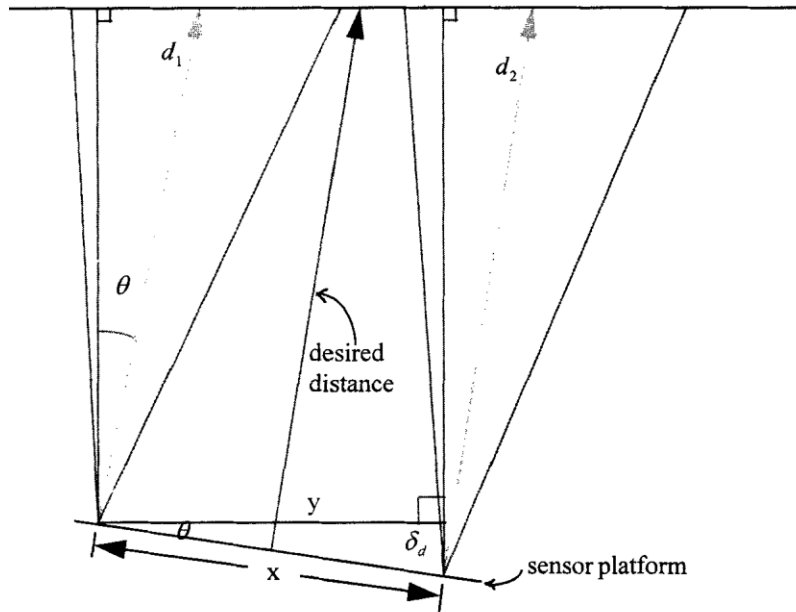


Figure 3.42: Ultrasonic sensor measurement model [21]

- (b) The Gaussian noise to environmental changes. There is an almost 3.5% increase in noise for a temperature difference of only 20^0 [21].

To use this approach requires calibration of many parameters, some of which are to be done in real time. A mathematical model would be preferable for this calibrations.

2. Load cells

These are transducers capable of converting pressure to an electrical signal specifically a strain in its material structure is converted to electrical resistance.

The loading cell disc shown in Figure 3.43 with a load force range of 0-50Kg was selected for application due to its weight range.



Figure 3.43: Strain-type load cells [22]

The use of a load cell was selected for this application based on the merits listed in the descriptions above. However, a single-load cell disc will be inefficient in measuring the weight of this load. Therefore, four load cells were selected to strategically position at the edges of the support frame of the discharge collection tank, as shown in Figure 3.44.

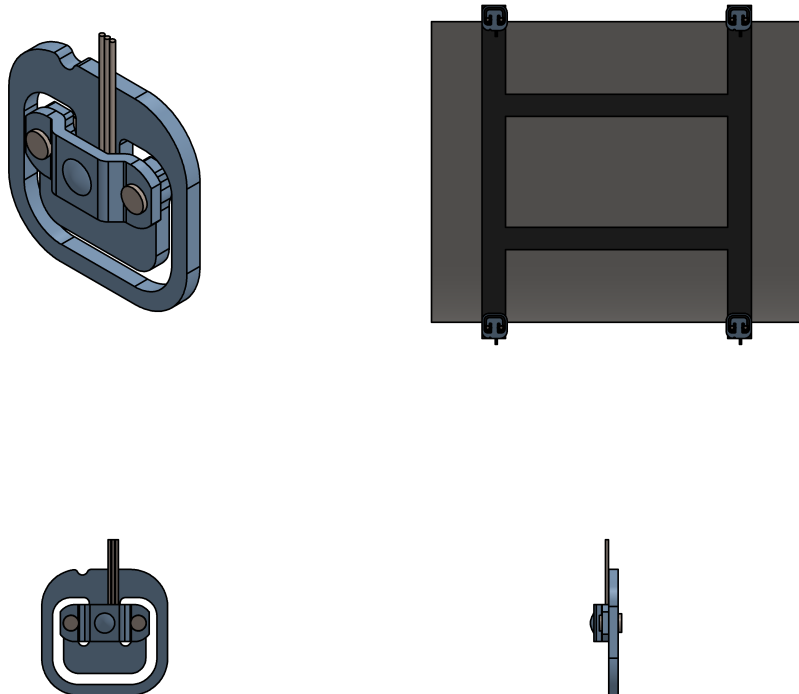


Figure 3.44: Collection tank with load cells

3.3.4 Temperature measurement sub-unit

In the same way as weight measurement of the discharge, the temperature of the discharge is measured in every step. This is relevant in ensuring consistency of the data collected in an experiment done in this machine.

Since this measurement is taken within roughly 10 seconds before the outlet valve is opened, a measuring device whose sensitivity is enough to establish reliable results within that time is required for this application.

A couple of temperature measurement sensors were considered for this application but an immersible DS18B20 temperature probe shown in figure 3.45 was selected. Its technical specifications are shown in table 3.5.



Figure 3.45: DS18B20 temperature probe [23]

Property	Value
Operating voltage	3.3V to 5V DC
Operating temperature range	-55°C to +125°C (-67°F to +257°F)
Accuracy over the range of -10°C to +85°C:	±0.5°C.
Water proof	True

Table 3.5: DS18B20 temperature range specifications [23]

3.3.5 Electrical

1. Solenoid valve connection

- **Power requirements**

The selected solenoid valve operates on 12V DC voltage. This requires an external supply and circuit to activate the supply when needed.

- **Circuit**

An IRF520 N-Ch power module described previously can be used to power this device with a 12V supply.

2. Strain type load cell connection

- **Power requirements**

The four load cells used in this application are connected through a load combinator module whose operating voltage is between 2.7V to 5V.

- **Circuit**

The load cells are connected in a Wheat-stone bridge through a load combinator module as shown in figure 3.46.

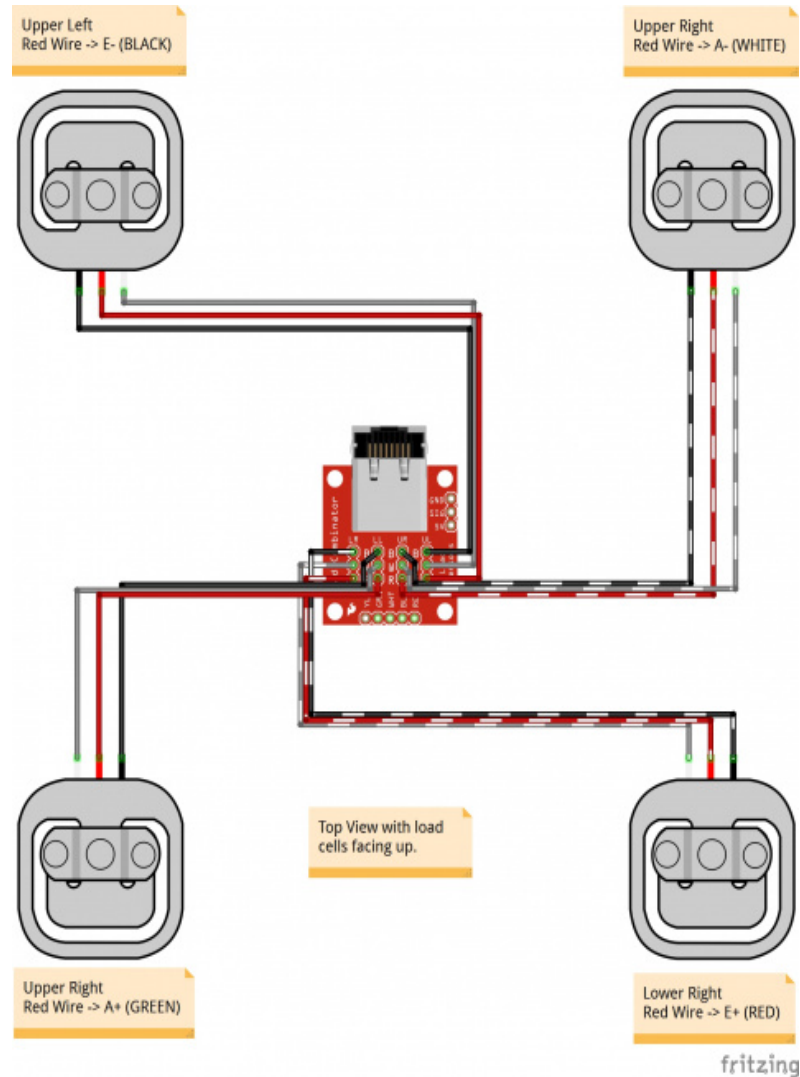


Figure 3.46: Load cells circuit [22]

3. DS18B20 temperature probe connection

- **Power requirements**

This sensor's operating voltage is between 3.0V and 5V. Therefore Vcc line can be connected directly to the 5V pin of the micro-controller.

3.3.6 Software and control

- **Calibration**

The load cells and the temperature sensor are calibrated once the whole system is assembled.

- **Auto calibration**

This can be achieved by having weight and temperature measurements triggered by an event and only measuring differential values.

- **Mean**

In this application, the weight and temperature of the discharge is measured over a period of time before the value of a measurement is determined. The noise in the variation within that time can be minimized by using a calibrated Kalman's filter.

3.4 Interface and Control Unit

This unit consists of two subunits:

1. Interface sub-unit
2. Controller sub-unit

3.4.1 Interface sub-unit

This sub-unit provides a means of interaction between the system and the user. Ideally, the subunit enables the user to input instructions and control the processes in this system. The status and results of processes in this system are also displayed in the interface. The choice of an interface depended on the following factors:

1. Size

This is the size of the operable part of the interface. In case of touch interface, a minimum of a 320x240 LCD is required to enable at least the minimum operability of GUI items, and a 20x4 LCD for any other choice.

2. Ergonomics

This refers to the impact of the interface on the user, the ease and efficiency in operating it. For an interface for this application, the user should be able to spend the least possible time feeding input and reading the results with relative ease.

3. Aesthetics

This is the perception of the user while operating the interface, their feeling about the interface. For this application, the interface will be used most frequently by students with limited exposure. A good look might be motivating. However, this should not compromise the design. It should be able to be introduced and improved with minimum modifications to the hardware in the system.

Based on the above considerations, the following options were considered:

1. LCD With keypad

This type of interface is shown in figure 3.47. One can navigate, read and provide input where it is required on the LCD display using the keypad.

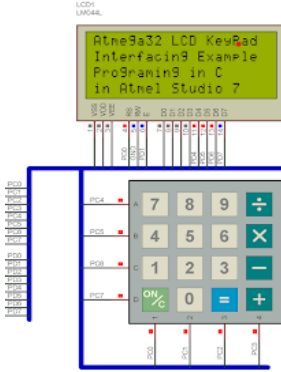


Figure 3.47: LCD with keypad [24]

2. LCD with touch

This type of interface is shown in figure 3.48. One can navigate such interface easily by touching or use a virtual keyboard to provide input.

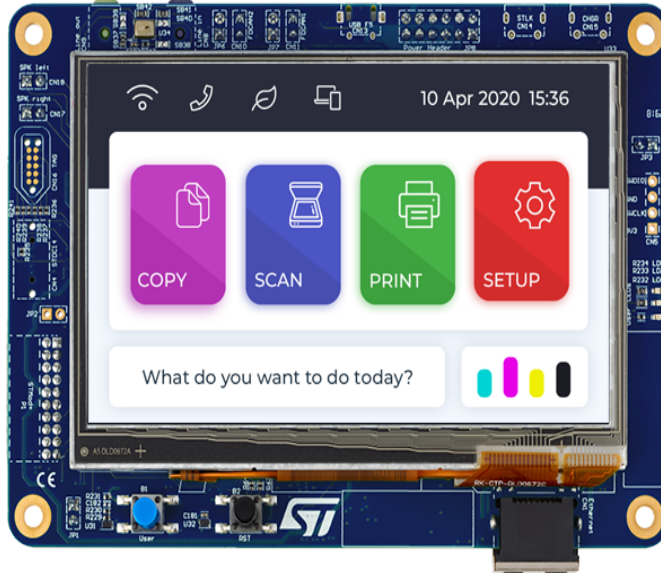


Figure 3.48: LCD with touch [25]

This type of LCD communicates with the microcontroller through an 8-bit parallel interface and four ports(32 pins). This can sometimes be replaced by an HDMI interface depending on the size of the screen.

3. LCD with Knob

This interface shown in Figure 3.49 is controlled by a knob. Navigation from page to page, field to field is achieved by turning the knob. To provide an input in a field, the knob can be pressed and turned. This is common in low-budget 3D printers.



Figure 3.49: LCD with knob [26]

An efficient choice for this application was to use a touch LCD interface. This choice satisfies all the requirements required of an interface for this application. In addition, one can also improve the aesthetics of the design by simply tweaking the GUI software without major hardware changes.

Touch LCDs can be very expensive relative to our budget and challenging to programme. Two variations of touch LCDs are available for our application: those with a 32-pin interface and those with an HDMI interface. Those with HDMI interface are available in sizes larger than 7 inches and are priced at not less than \$90. Those with 32-pin interface are available to sizes as small as 1.77 inches and are relatively cheaper.

- **LCD GUI design**

A preliminary GUI is shown in Figure 3.50.

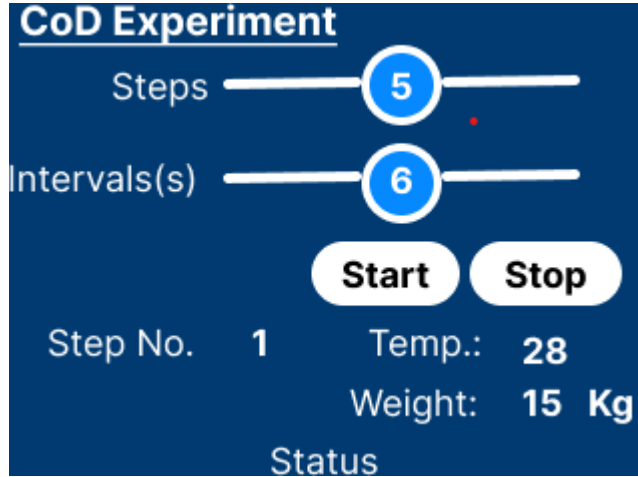


Figure 3.50: GUI interface

The design is in a 320x240 frame, the size of the selected LCD. The steps sizes and time interval's inputs can be provided by sliding on the sliding bar. The value of a position on the slider is displayed inside the slider handle.

The step number, weight and temperature of that specific step are also displayed once a step is complete.

In case of any errors in the system, an error message is displayed at the bottom of the frame.

3.4.2 Controller sub-unit

This sub-unit executes the application logic, sends instructions to the actuators, and reads inputs from sensors in the system. It is responsible for synchronising the GUI with the processes in the hardware. This unit monitors and controls the parameters of the input devices and generates output signals to implement desired tasks.

The choice of a micro-controller for this application was guided by the selected interface, a touch LCD. Figure 3.51 shows the selection procedure for a micro-controller for this application.

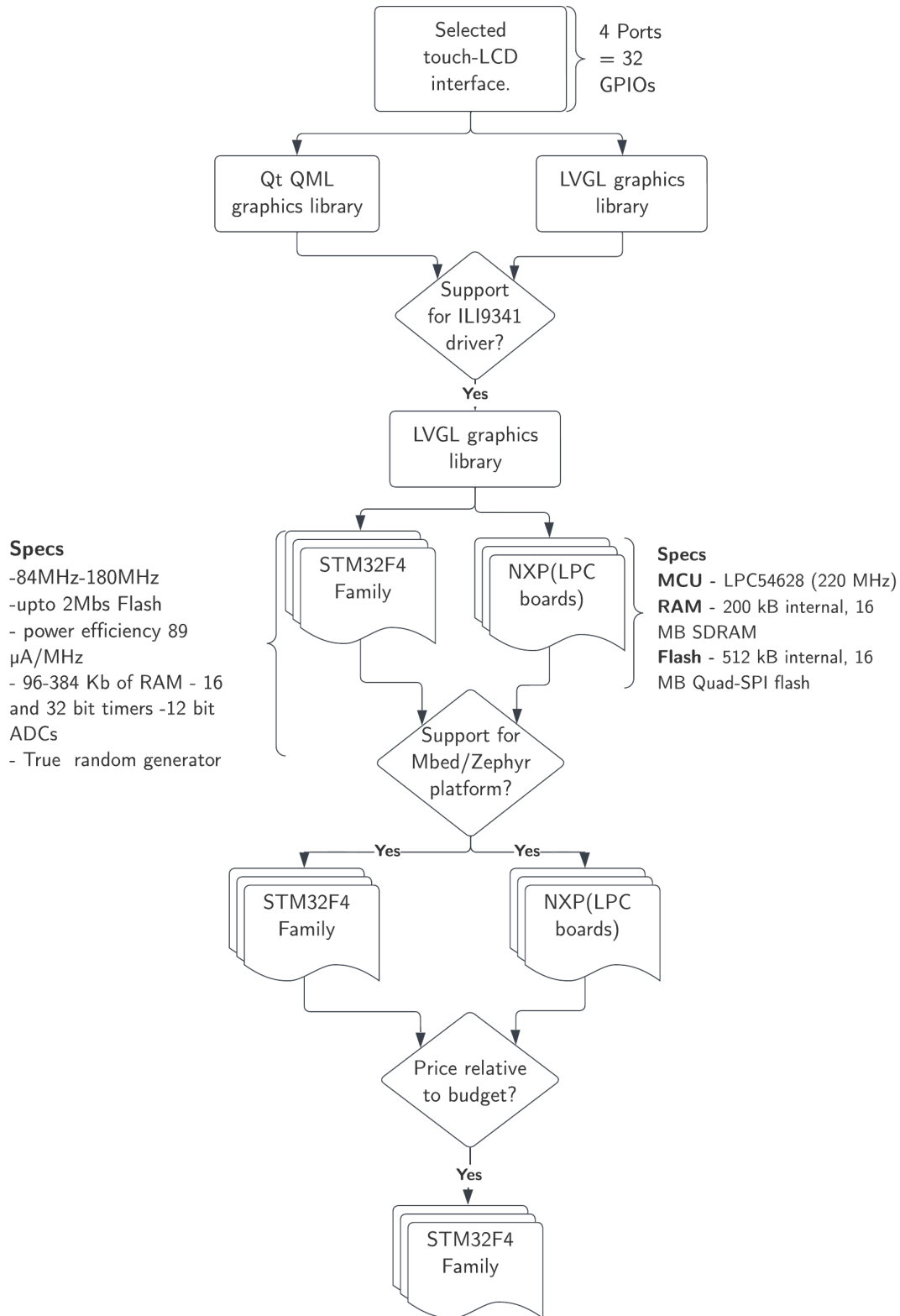


Figure 3.51: Board Selection

- **Graphics library**

To develop graphics for a touch LCD, the choice of graphics libraries was between the Light and Versatile Embedded Graphics Library (LVGL) and the Qt/QML graphics libraries. These two are versatile and have great community support. Each library supports specific display drivers out-of-the-box. For this application, an LCD with an ILI9341 driver had been selected, therefore support for this specific driver was necessary. Drivers for a specific driver could also be developed from scratch in a long and tedious process. To avoid this, out-of-the-box support was required. LVGL tends to offer that support; therefore, it was selected as the graphics library for this application.

- **Board support**

LVGL library also provides support for specific board families out of the box, such as the NXP and STM32F4 families. LVGL support for these boards automatically means that this board has the number of ports required for LCD touch functionality.

- **Platform support**

LVGL is just a graphics library. The board is required to support other peripherals such as the electromagnet, servo motor, weight and temperature measurement devices, and the solenoid valve. This can be done in an RTOS platform such Zephyr(C/C++) or Mbed(C++). However, these platforms support specific boards out-of-the-box, but custom boards could also be added. To make the project a little easier, an out-of-the-box was required. The two platforms tend to support the two boards.

- **Price**

This is the most crucial part of this selection. Both boards can be considered expensive relative to the project's budget, but the STM32F4 family boards can be relatively cheaper. Therefore, an STM32F407VET6 board was selected.

3.4.3 Electrical

- **Touch LCD connection**

STM32F407VET6 board provides a dedicated interface for touch LCD with FSMC interface as shown in figure 3.53.

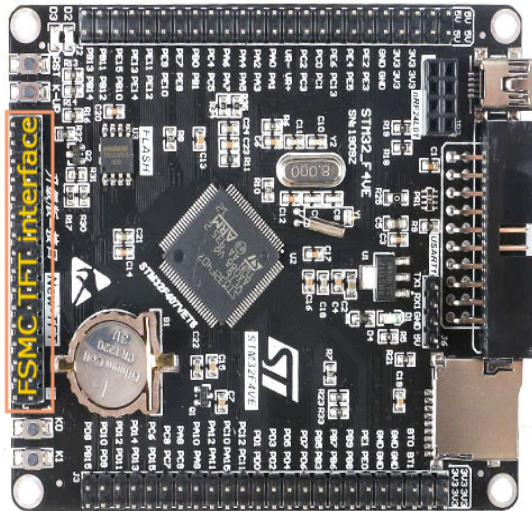


Figure 3.52: FSMC interface in STM32F407VET6 [27]



Figure 3.53: STM32 connected with LCD [27]

3.4.4 Software and control

The logic of the whole application is shown in figure 3.54.

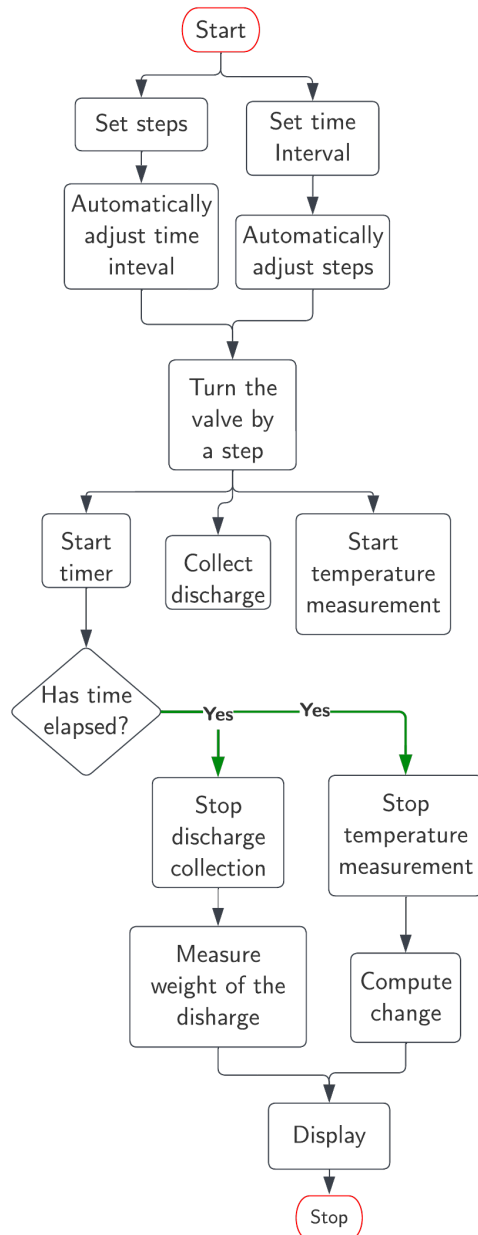


Figure 3.54: Application logic

The application requires the user to set the number of steps of the experiment or the time interval between the steps. This is done by sliding the slide handle of one of the inputs in the touch GUI. When the user presses the handle on the input of the steps, the system automatically adjusts the time interval between the steps and vice versa.

Once the steps are set, the user clicks on the start button. The system then turns the valve by one step after starting the timer. This is done simultaneously with commencement of the discharge collection and the measurement of the discharge temperature.

The system will continuously check if the time interval has elapsed and if it has, it will simultaneously stop the discharge collection and the temperature measurement. It will then compute the differential change in temperature and measure the weight of the discharge. The results of this measurement are displayed in the GUI.

This is repeated for the set steps but the user has the option to cancel the experiment.

4 Results

This section contains the results obtained during the design of the three units of the project.

4.1 Discharge Flow Control Unit

4.1.1 Flow control sub-unit

An MG996R servo motor was selected for this sub-unit, to open and close the valve in steps that can be less than 1° depending on the number of steps requested by the user. Direct pulse width modulation was preferred to a micro-step drive as a mechanism to drive the servo motor in steps of any size.

A mounting mechanism for the servo motor was designed to the specs of the motor and stress-tested. It was found to withstand the maximum torque of the motor.

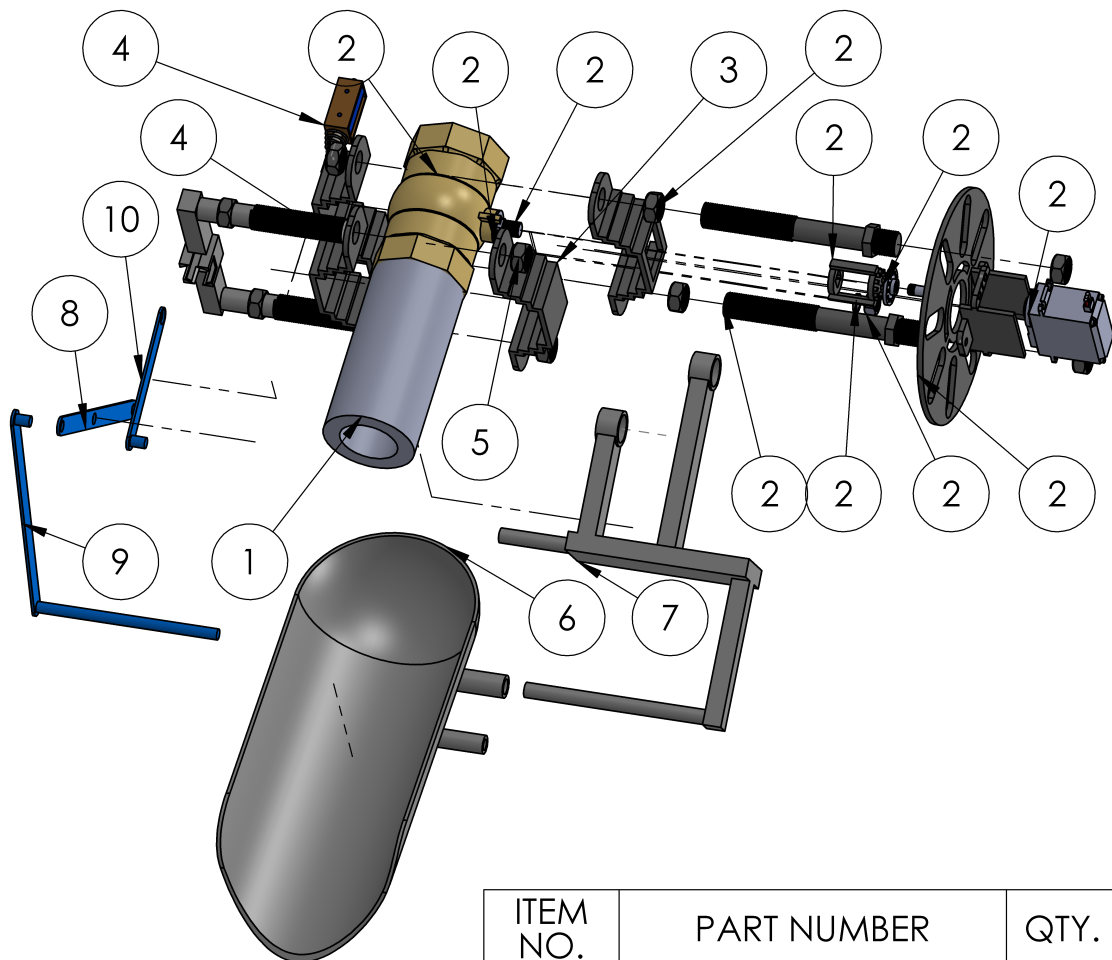
4.1.2 Flow diversion sub-unit

A P16-S micro-linear actuator with a linear stroke length of 100mm and stroke-speed of 150mm/s was selected to operate a flap used to divert the discharge flow either into the main reservoir or the discharge collection tank.

A four-bar kinematic chain was designed and simulated in MechDesigner based on the motion required for the flap. The chain achieved the motion based on the cam data obtained from the simulation.

4.1.3 Unit Assembly

The assembly of the discharge flow control unit is shown in figure 4.1.



ITEM NO.	PART NUMBER	QTY.
1	Pipe Extension	1
2	Servo Support frame	1
3	two Rail Straps Bottom	2
4	Electromagnet Assem bly	1
5	Straps Nut	4
6	flap	1
7	Diversion Support	1
8	Coupler	1
9	Rocker	1
10	Crank	1

Figure 4.1: Unit Exploded view

From a motion study simulation in SolidWorks, the assembly appears to be able to regulate the fluid flow in steps as per the users specifications. The diversion unit also seems to be able to divert the flow either to the main reservoir or to the discharge collection tank.

4.2 Discharge Flow Handling unit

4.2.1 Discharge collection tank sub-unit

A horizontal half-cylindrical tank was preferred to a cuboid tank from a simulation that showed that the pressure of the collected fluid will concentrate on a line at the bottom of the tank. This is preferred in this application in order to minimize the time taken to empty the tank.

4.2.2 Outlet valve sub-unit

A solenoid valve was preferred to a butterfly valve because of its relatively cheaper price though the preferred size is slower.

4.2.3 Weight measurement sub-unit

Four load cells connected on a Wheatstone bridge were preferred to an ultrasonic approach to measure the weight of the collected discharge because the ultrasonic approach is unreliable.

4.2.4 Temperature measurement sub-unit

A DS18B20 immersible temperature sensor was selected for this subunit due to its reliability and sensitivity.

4.2.5 Final assembly

Figure 4.2 shows the designed system attached to the Synthetic Hydro-Experimental Machine currently in use in JKUAT.

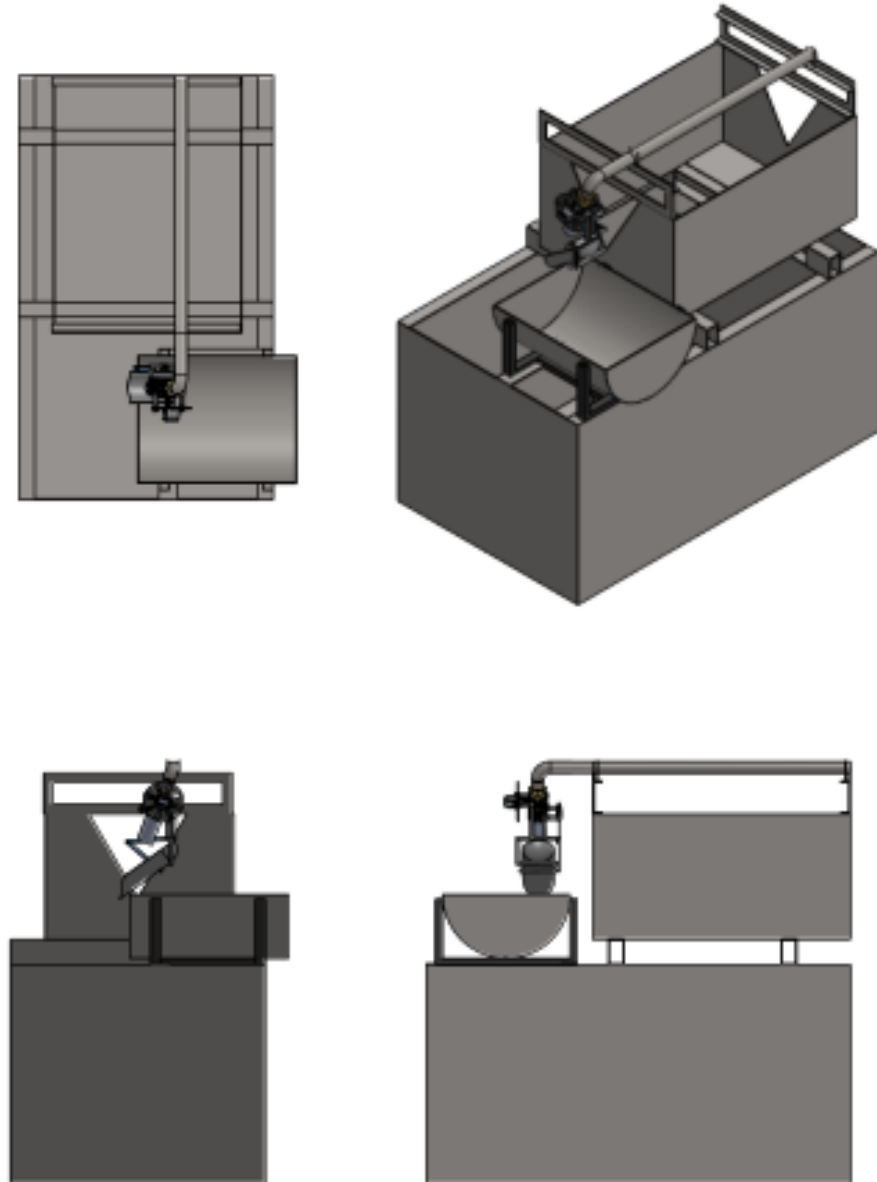


Figure 4.2: Final Assembly

The dimensions of the part are derived from the existing machine.

4.3 Budget

The table 4.1 shows the budget of the project.

Item No.	Item	Description	Unit Cost	No.	Total Cost
1	Servo Motor	MG996R(4.8Kg/cm)	800	1	800
2	Linear Actuator	P16-S Linear Actuator	3500	1	3500
3	Load cells	50 Kg Load cells	150	4	600
4	Load cell Amplifier	HX711	100	1	100
5	Temperature Sensor	DS18B20 Immersible	300	1	300
6	Solenoid valve	3/4" Plastic	900	1	900
7	MCU	STM32F407VET6	4400	1	4400
8	LCD	320x240 Touch LCD	1200	1	1200
9	Power MOSFET	IRF520 N-ch	550	3	1650
10	Voltage Regulator	XL4015 DC-DC adjustable buck module	400	3	1200
11	Transformer	AC 220V TO DC 12V 5A Transformer Power Supply	1100	1	1100
12	Fabrication Cost	3D printing & Others	10000	1	10000
Total					22600

Table 4.1: Budget

5 Conclusion

The objective of this project was to design and fabricate an automated discharge collection process which entailed the design of the discharge flow control unit, the discharge collection unit, the electrical and electronic and the control algorithm which were clearly met. This phase only involved the design work which has been done conclusively.

The next phase to be implemented will involve the fabrication of the developed design. However, it is expected that during this phase, few modifications and redesigns will have to be done to further optimize the design.

References

- [1] M. Pereira, “Flow meters: part 1,” *IEEE Instrumentation & Measurement Magazine*, vol. 12, no. 1, pp. 18–26, 2009.
- [2] P. Nandagopal and S. Nuggenhalli, “Fluid flow measurements,” pp. 137–147, 2022.
- [3] R. K. Raman, Y. Dewang, and J. Raghuwanshi, “A review on applications of computational fluid dynamics,” *International Journal of LNCT*, vol. 2, no. 6, pp. 137–143, 2018.
- [4] A. Tukimin, M. Zuber, and K. Ahmad, “Cfd analysis of flow through venturi tube and its discharge coefficient,” in *IOP Conference Series: Materials Science and Engineering*, vol. 152, no. 1. IOP Publishing, 2016, p. 012062.
- [5] M. Carello, A. Ivanov, and F. Pescarmona, “Flow rate test bench: automated and compliant to iso standards,” *Experimental Techniques*, vol. 37, no. 2, pp. 41–49, 2013.
- [6] N. Tamhankar, A. Pandhare, A. Joglekar, and V. Bansode, “Experimental and cfd analysis of flow through venturimeter to determine the coefficient of discharge,” *International Journal of Latest Trends in Engineering and Technology (IJLTET)*, vol. 3, no. 4, pp. 194–200, 2014.
- [7] “Venturi Flowmeter.” [Online]. Available: <http://hyperphysics.phy-astr.gsu.edu/hbase/Fluids/venturi.html>
- [8] R. Arun, K. Yogesh Kumar, and V. Seshadri, “Prediction of discharge coefficient of venturimeter at low reynolds numbers by analytical and cfd method,” *International Journal of Engineering and Technical Research (IJETR) ISSN*, pp. 2321–0869, 2015.
- [9] A. Odetti, G. Bruzzone, M. Caccia, R. Ferretti, E. Spirandelli, and G. Bruzzone, “Design, development and testing at field of a modular mini automatic water sampler (maws) based on magnetic activation,” in *OCEANS 2019-Marseille*. IEEE, 2019, pp. 1–8.

- [10] S. Lee and J. Kim, “Development and characterization of a cartridge-type pneumatic dispenser with an integrated backflow stopper,” *Journal of Micromechanics and Microengineering*, vol. 20, no. 1, p. 015011, 2009.
- [11] L. Warguła, P. Krawiec, J. M. Adamiec, and K. J. Waluś, “The investigations of dynamic characteristics of a stepper motor,” *Procedia Engineering*, vol. 177, pp. 318–323, 2017.
- [12] “NEMA 17 Stepper Motor.” [Online]. Available: <https://components101.com/motors/nema17-stepper-motor>
- [13] R. Halicioglu, L. C. Dulger, and A. T. Bozdana, “Mechanisms, classifications, and applications of servo presses: a review with comparisons,” *Proceedings of the Institution of Mechanical Engineers, Part B: Journal of Engineering Manufacture*, vol. 230, no. 7, pp. 1177–1194, 2016.
- [14] “MG996R Servo Motor.” [Online]. Available: <https://components101.com/motors/mg996r-servo-motor-datasheet>
- [15] X. Gao, J. Yang, J. Wu, X. Xin, Z. Li, X. Yuan, X. Shen, and S. Dong, “Piezoelectric actuators and motors: materials, designs, and applications,” *Advanced Materials Technologies*, vol. 5, no. 1, p. 1900716, 2020.
- [16] admin, “High Precision Stages And Actuators.” [Online]. Available: <https://xeryon.com/products/>
- [17] “P16 Mini Linear Actuators - Actuonix Motion Devices.” [Online]. Available: <https://www.actuonix.com/p16>
- [18] “Using IRF520 MOSFET Switch button for Arduino - Robojax.” [Online]. Available: <https://robojax.com/learn/arduino/?vid=robojax-IRF520-MOSFET>

- [19] “butterfly valve 250mm - Buy butterfly valve 250mm Product on FLOWX Valve.” [Online]. Available: <http://www.flowxcontrol.com/butterfly-valve-250mm-pd91762826.html>
- [20] “1/2” 12V DC Electric Brass Solenoid Valve 12-Volts.” [Online]. Available: <https://www.electricsolenoidvalves.com/1-2-12v-dc-electric-brass-solenoid-valve/>
- [21] C. C. Chang and K.-T. Song, “Ultrasonic sensor data integration and its application to environment perception,” *Journal of Robotic Systems*, vol. 13, no. 10, pp. 663–677, 1996.
- [22] “Getting Started with Load Cells - learn.sparkfun.com.” [Online]. Available: <https://learn.sparkfun.com/tutorials/getting-started-with-load-cells/all>
- [23] “DS18B20 Temperature Sensor.” [Online]. Available: <https://components101.com/sensors/ds18b20-temperature-sensor>
- [24] “Electronics and Programming: ATMega32 LCD and Keypad Interfacing Example.” [Online]. Available: <https://aki-technical.blogspot.com/2021/05/atmega32-lcd-and-keypad-interfacing.html>
- [25] “For developers - Get started now | LVGL.” [Online]. Available: <https://lvgl.io/developers>
- [26] “Prusa i3 MK2 / MK3 LCD Knob Round (depth corrected) by amoose136 | Download free STL model.” [Online]. Available: <https://www.printables.com/model/76087-prusa-i3-mk2-mk3-lcd-knob-round-depth-corrected>
- [27] “Black STM32 F407VE Development Board — Zephyr Project Documentation.” [Online]. Available: https://docs.zephyrproject.org/3.1.0/boards/arm/black_f407ve/doc/index.html

A Appendix

A.1 Semester 1 Time Plan

Week	1	2	3	4	5	6	7	8	9	10	11
Project proposal											
Continous Presentation											
Literature review											
Discharge flow control design											
Discharge collection unit design											
Interface and control design											
Assembly and testing											
Interim report											
Final presentation											

Table A.1: Semester 1 timeplan

Table A.2: Semester 2 Timeplan

A.2 Semester 2 Time Plan

A.3 P16-S Micro linear actuator

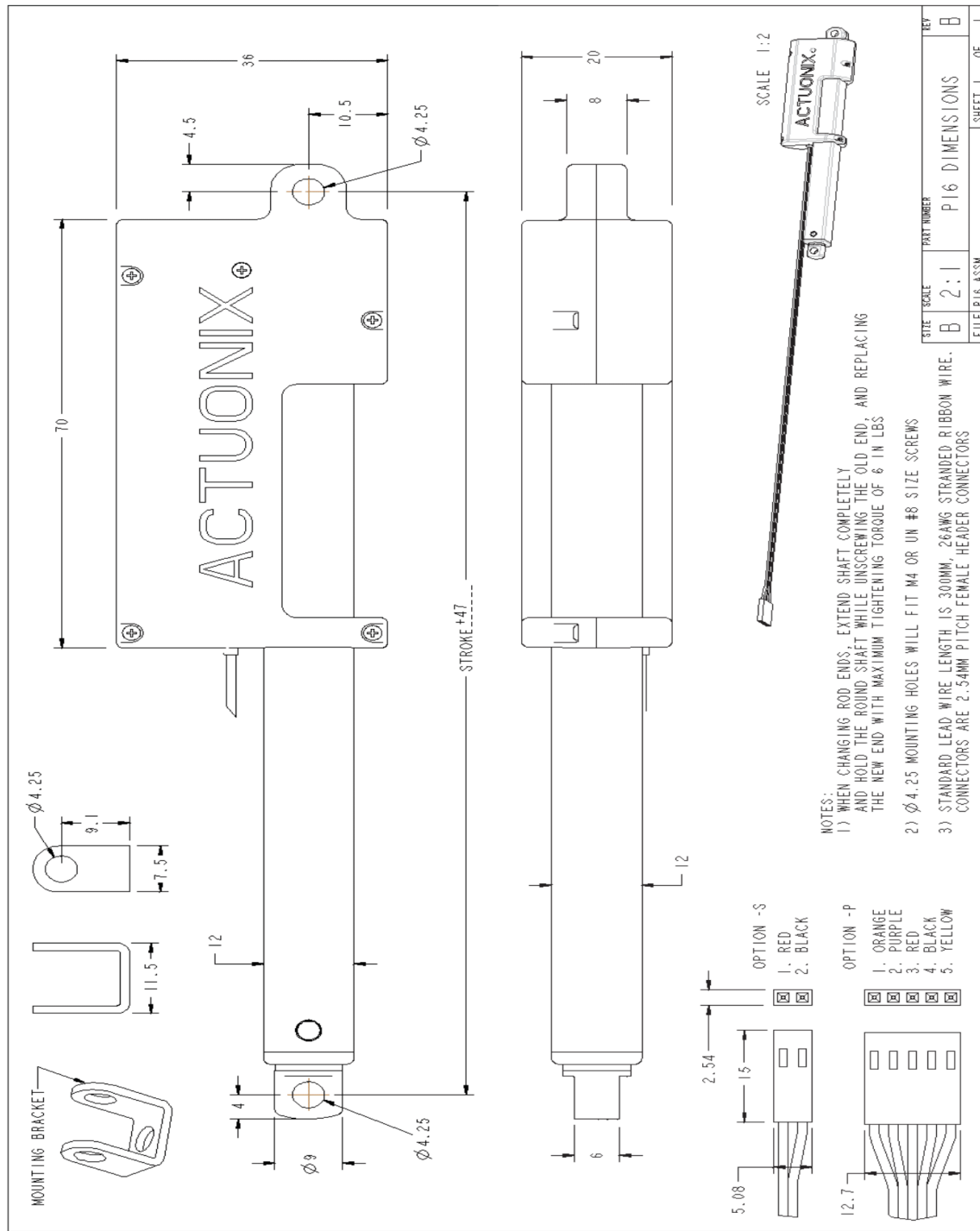


Figure A.1: P16-S Micro linear actuator dimensions

A.4 Synthetic Hydro Experimental Machine in JKUAT

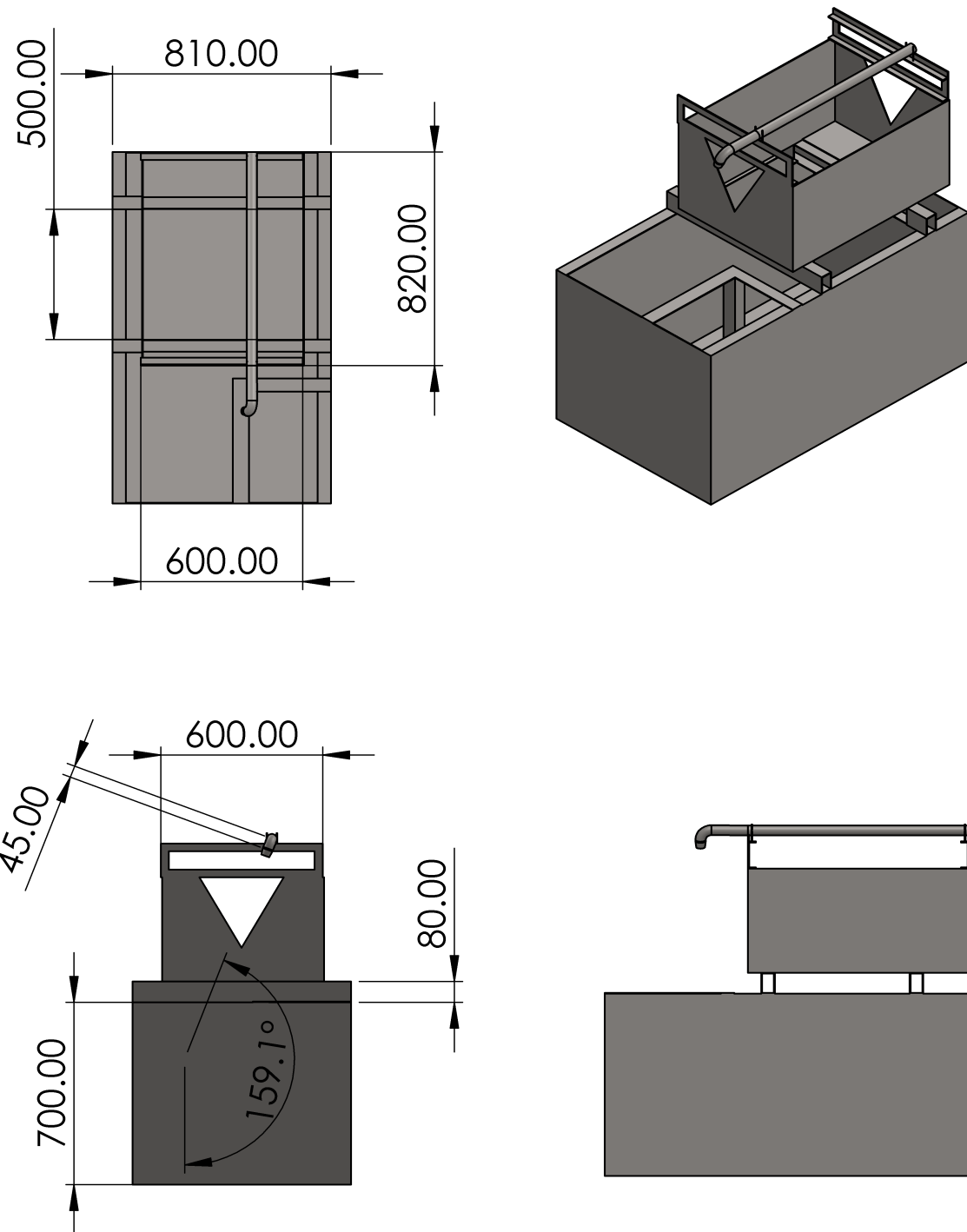


Figure A.2: S.H.E.M relevant machine dimensions